



Article

Identifying the Factors behind Climate Diversification and Refugial Capacity in Mountain Landscapes: The Key Role of Forests

Raúl Hoffrén ^{1,2} , Héctor Miranda ¹ , Manuel Pizarro ¹ , Pablo Tejero ¹ and María B. García ^{1,*}

¹ Pyrenean Institute of Ecology, Spanish National Research Council (IPE-CSIC), Av. Montañana 1005, 50059 Zaragoza, Spain; rhoffren@unizar.es (R.H.); hmiranda@ipe.csic.es (H.M.); m.pizarro@csic.es (M.P.); ptibarra@ipe.csic.es (P.T.)

² Geoforest-IUCA, Department of Geography and Land Management, University of Zaragoza, Cl. Pedro Cerbuna 12, 50009 Zaragoza, Spain

* Correspondence: mariab@ipe.csic.es; Tel.: +34-976-369-393 (ext. 880051)

Abstract: Recent studies have shown the importance of small-scale climate diversification and climate microrefugia for organisms to escape or suffer less from the impact of current climate change. These situations are common in topographically complex terrains like mountains, where many climate-forcing factors vary at a fine spatial resolution. We investigated this effect in a high roughness area of a southern European range (the Pyrenees), with the aid of a network of miniaturized temperature and relative humidity sensors distributed across 2100 m of elevation difference. We modeled the minimum (T_n) and maximum (T_x) temperatures above- and below-ground, and maximum vapor pressure deficit (VPD_{max}), as a function of several topographic and vegetation variables derived from ALS-LiDAR data and Landsat series. Microclimatic models had a good fit, working better in soil than in air, and for T_n than for T_x. Topographic variables (including elevation) had a larger effect on above-ground T_n, and vegetation variables on T_x. Forest canopy had a significant effect not only on the spatial diversity of microclimatic metrics but also on their refugial capacity, either stabilizing thermal ranges or offsetting free-air extreme temperatures and VPD_{max}. Our integrative approach provided an overview of microclimatic differences between air and soil, forests and open areas, and highlighted the importance of preserving and managing forests to mitigate the impacts of climate change on biodiversity. Remote-sensing can provide essential tools to detect areas that accumulate different factors extensively promoting refugial capacity, which should be prioritized based on their high resilience.

Keywords: LiDAR; Landsat; microclimate; thermal stability; vegetation structure; topography



Citation: Hoffrén, R.; Miranda, H.; Pizarro, M.; Tejero, P.; García, M.B. Identifying the Factors behind Climate Diversification and Refugial Capacity in Mountain Landscapes: The Key Role of Forests. *Remote Sens.* **2022**, *14*, 1708. <https://doi.org/10.3390/rs14071708>

Academic Editor: Henning Buddenbaum

Received: 28 February 2022

Accepted: 29 March 2022

Published: 1 April 2022

Publisher's Note: MDPI stays neutral with regard to jurisdictional claims in published maps and institutional affiliations.



Copyright: © 2022 by the authors. Licensee MDPI, Basel, Switzerland. This article is an open access article distributed under the terms and conditions of the Creative Commons Attribution (CC BY) license (<https://creativecommons.org/licenses/by/4.0/>).

1. Introduction

Halting the loss of biodiversity resulting from current global change is one of the main challenges we face for the conservation of a healthy planet. Although there is clear evidence of its effect on all facets of nature [1,2], we still have a significant lack of knowledge about where it is having the strongest or mildest impact. As an example, while global warming is often considered especially detrimental in mountains and alpine landscapes (e.g., [3,4]), some studies claim the contrary. At a large scale, Loire et al. (2009) [5] and Sandel et al. (2011) [6] described lower climate change velocity in mountains and forecasted that they may effectively shelter many species into the next century. At a finer scale, Scherrer and Körner (2010, 2011) [7,8] demonstrated that alpine landscapes harbor temperature mosaics that provide more refugia for plants than lowland areas. Moreover, Suggitt et al. (2018) [9] recently unveiled that the microclimatic heterogeneity typical of mountains had buffered population losses for insects and plants caused by climate change across England. These studies showcase the difficulty of translating the real effect of climate change from large-scale theoretical or predictive models to local scenarios.

Topographically complex areas like mountains include many climate-forcing factors at a fine spatial resolution [10,11] such as terrain features that reduce solar radiation (e.g., slope, aspect) and landforms that favor humidity stability or accumulation of cold air (e.g., canyons) (e.g., [12,13]). In addition, mountains are covered by different patches of vegetation, and living under the tree canopy means experiencing damped extreme temperatures (lower maximums and higher minimums), as well as lower direct sunlight and wind speed [14,15]. However, microclimatic conditions under the canopy in terms of temperature, light, and humidity will depend on the forest structure (tree density, canopy height) and topographic position (e.g., [16–18]). Topographic and vegetation factors, therefore, introduce local diversification into the regional matrix of temperatures and moisture, and make mountains well-suited for the existence of climatic microrefugia: areas buffered from contemporary climate change due to their lower exposure to extreme temperatures and external fluctuations, which favor the persistence of certain organisms [19–21]. High climatic diversity will allow species to move across short distances to avoid the detrimental effects of short-term climate warming, while thermally stable areas will provide refuge thanks to their lower sensitivity to extreme events. Therefore, given that climate change impacts will be less prevalent for organisms in those sites [22,23], obtaining an accurate picture of microclimates across landscapes over large areas and the factors underlying such diversification allow for an assessment of their current refugial capacity, to mitigate the impact of anthropogenic climate change on biodiversity [24]. This type of analysis can help prioritize the protection of the best places as refugia, those that are likely to offer the greatest opportunities for biodiversity to persist [25,26].

Detecting microclimatic diversity, however, requires measuring or accurately estimating temperatures at a local scale, which can vary greatly in space. Near-ground extreme temperatures are the ones critical for small or sedentary (micro-)organisms on the surface and at the subsurface level, for processes like germination or survival, and thus for the assemblage of plant and animal communities (e.g., [27]). Those temperatures can strongly deviate from the ones interpolated from meteorological stations with sensors located at a 1.5–2 m height in open landscapes, as well as from temperatures provided by satellite imagery due to their coarse resolution ($\sim 1 \text{ km}^2$). Therefore, climatic information aimed at studying the effect of global warming on biodiversity should be recorded near organisms whose presence depends on physiological limitations associated with temperature. The availability and easy use of miniaturized sensors with dataloggers have promoted recent studies on fine-scale microclimatic conditions in very contrasted and complex regions (e.g., [28–32]), as well as a worldwide network to compile and analyze microclimatic information [33]. In parallel, new technologies based on remote-sensing such as thermal cameras or LiDAR (Light Detection and Ranging) make it possible to map thermal landscapes and vegetation structures with unprecedented levels of accuracy and resolution [8,34,35], allowing analyses to associate the effect of terrain and habitat structure on the microclimate [36–38]. As a result, fine-resolution topographic and vegetation metrics, together with information provided by climatic sensors, are becoming a powerful tool to describe thermal variability across complex areas and to detect potential microrefugia [18,34,39].

The aim of this study is to show the variety of microclimates held in a small and rugged mountain area, and analyze the relative importance of environmental factors for climate diversification and the sheltering capacity at a local scale. We explore fine-grained variability in above- and below-ground temperatures (T) and vapor pressure deficits (VPDs; the evaporative demand of the air that drives transpiration) across a mountain landscape of the Pyrenean range that covers 2100 m of elevation difference: the Ordesa and Monte Perdido National Park (PNOMP). We focus on extreme temperatures of air and soil (minimum: T_n ; maximum: T_x), as well as the maximum vapor pressure deficit (VPD_{max}), because climate extremes have shaped the contemporary distributions of plant species [40] and constitute thresholds for the biological activity across a range of taxonomic diversity: edaphic microbiota, plants (above-ground parts and roots), invertebrates, and vertebrates. By combining terrain and vegetation variables obtained from remote-sensing active sen-

sors (ALS-LiDAR) and optical imagery (Landsat), as well as microclimatic measurements recorded in the field with miniaturized sensors, we first quantify the role of topographic variables, vegetation, and the forest structure on above- and below-ground T_n and T_x , and VPD_{max} , and then we analyze the thermal stability (ST) and decoupling from macroclimate temperatures (offsets). Our goal is to answer the following questions: (1) What topographic and vegetation factors have a strong effect on T_n , T_x , and VPD_{max} in the area, and what role do forests play, in particular? (2) Is the strength of these factors consistent above- and below-ground, for T_n and T_x , and across the years? and (3) Which factors promote refugial capacity in terms of narrowing the thermal niche (high thermal stability) or offsetting free-air extreme temperatures? We finally discuss to what extent information on terrain features and the vegetation structure derived from remote sensors can be used to guide management actions for preserving biodiversity more efficiently in the face of climate warming.

2. Materials and Methods

2.1. Study Area

The study was conducted in the central sector of the Pyrenean mountains, at the Ordesa and Monte Perdido National Park and its peripheral zone (PNOMP thereafter, Figure 1). This area extends over 350 km² and is characterized by its high roughness and elevation range: from the 660 m a.s.l. of the Añisclo Canyon to the 3355 m a.s.l. of the Monte Perdido summit, the highest calcareous massif in Europe. The topographic profile comprises five deep valleys radiating from it: Bujaruelo, Ordesa, Añisclo, Escuin, and Pineta (Figure 2). The basis of its current morphology dates back to the Alpine Orogeny, which caused the uplift of Paleozoic materials and shaped the greatest entity reliefs. Among the geomorphological components of greater presence are glacial and periglacial modeling, which are the result of the glacial-interglacial alternate periods of the Quaternary. Fluvial modeling is also very relevant due to the intense erosive activity that river flows have exerted on the PNOMP's karstic materials. Most of the region covers the montane and subalpine elevation ranges, and vegetation types include a variety of forests and grasslands. The topographic complexity, heterogeneous exposition of its valleys and canyons, and its southern peripheral position during the glaciations have promoted remarkable biodiversity: the area harbors about 1400 vascular plants, i.e., about one-tenth of the whole European flora [41].

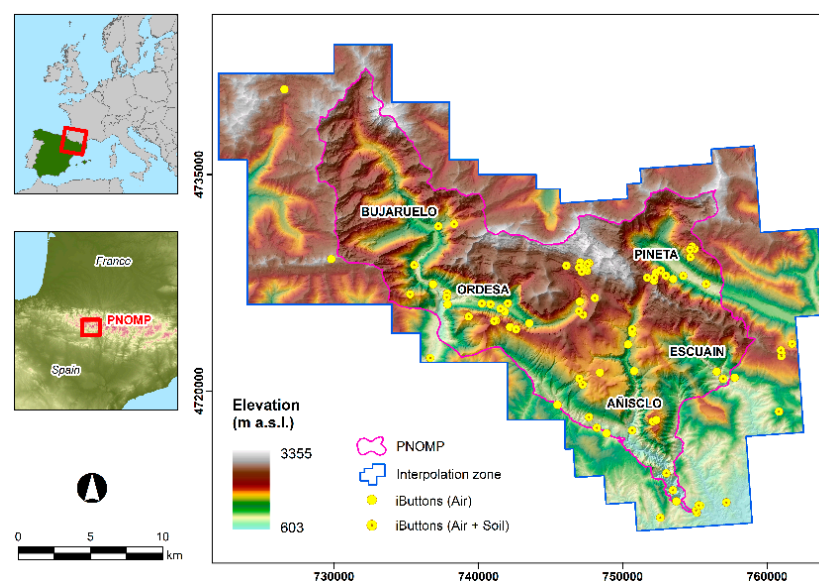


Figure 1. Study area on the south side of the Central Pyrenees: the Ordesa and Monte Perdido National Park (PNOMP), and its five valleys included. The yellow circles indicate the distribution of the iButtons to measure temperatures and relative humidity.

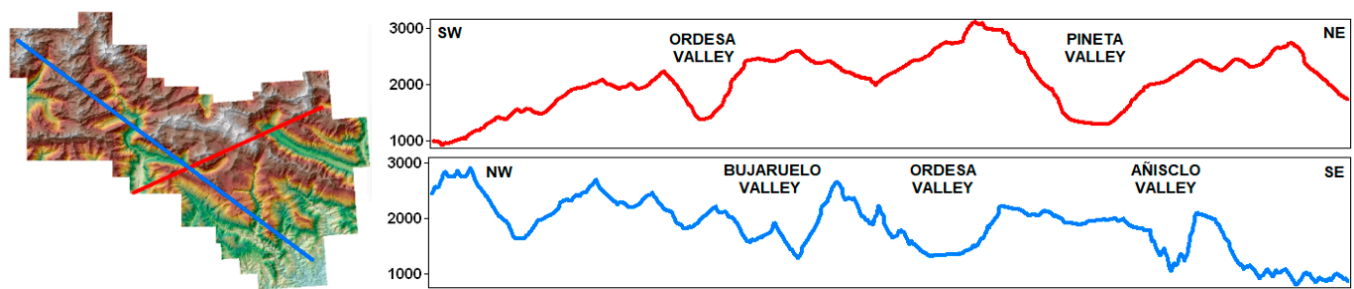


Figure 2. Two different topographic profiles in the study area (PNOMP), showing the rugosity and alternance of high mountains with canyons and valleys.

2.2. Macro- and Microclimate Data Acquisition

Fine-scale above-ground (air) and below-ground (soil) temperatures and relative air humidity metrics (“microclimate”) were obtained across a network of miniaturized sensors distributed over the heterogeneous landforms of the National Park and surroundings, considering habitat representativeness and accessibility for frequent downloading (a few were placed outside, in the “interpolation zone”, to reduce the important boundary effect of the PNOMP star-like shape; Figure 1). A wide variety of environments were selected: fir forests, Scots pinewoods, forests of mountain pine, beech and mixed forests, riparian, marcescent oak woods, Mediterranean oak woods, shrublands, subalpine grasslands, and screes. We initially chose 100 sites: 21 deciduous forests located between 664 and 1906 m a.s.l., 21 evergreen forests between 680 and 2084 m a.s.l., and 58 open areas between 660 and 2720 m a.s.l (both Mediterranean and subalpine shrublands, grasslands, and screes). This network of sensors covered about 2100 m of elevation, contrasted vegetation formations, topographic exposure, slope, and radiation (Figure 3).

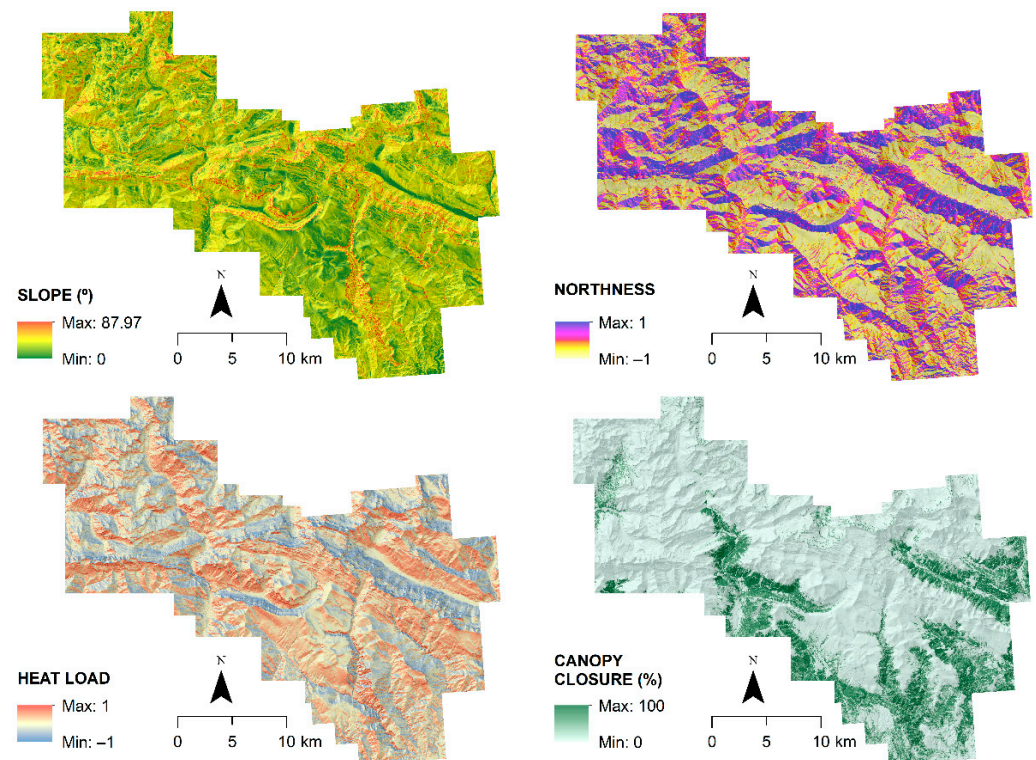


Figure 3. Topographic and environmental variability in the study area, corresponding to 4 of the 11 variables analyzed in this study: slope, northness, heat load, and canopy closure.

At each site, we installed two kinds of sensors with loggers (iButton® model, Maxim Integrated). They allow us to detect fine-scale temporal series of the microclimatic condi-

tions at any place, and have been widely used to identify microclimates and microrefugia in very contrasted environments [42]. A Hygrochron (DS1923) was placed above the surface (air sensors), and with 57 of them, we also placed a Thermochron (DS1920) below the surface (soil sensors). The former were shielded with a white mesh to avoid overheating while allowing wind flow. The latter was wrapped with tape to avoid failures due to soil moisture. Since our intention was to capture the overall temperatures where most organisms are found, we placed sensors to record near-ground temperatures in open habitats at about 5 cm height, and overall temperatures within forests at 1.2 m height. Soil sensors were placed at a depth of 5–10 cm, which is a critical layer for plant roots and provides habitats for many invertebrates and microbiota.

Sensors recorded every 4 h, starting at 12 a.m. solar time, from which we calculated the daily T_n and T_x. Both temperature (T, in °C) and relative humidity (RH, in %) were visually and quantitatively checked for potential errors (see below). The VPD (in kPa) was calculated from the algorithm that combines T and RH (Equations (1) and (2); see [27]) as the difference between the saturation and actual vapor pressure for each temperature record:

$$e_s = 0.6112 \times \exp[(17.67 \times T)/(T + 243.5)] \quad (1)$$

$$\text{VPD} = [(100 - \text{RH})/100] \times e_s \quad (2)$$

Free-air climatic metrics (monthly minimum and maximum T) were acquired from WorldClim database v.2 [43] across the surface of the PNOMP. WorldClim provides values in a gridded surface of 1 km² resolution from 1970 to 2000. Thereafter, we will refer to it as the “macroclimate”. We used a worldwide database because there is only one meteorological station in the study area (Góriz, located at 2200 m a.s.l.).

2.3. Microclimatic Data-Processing

Measurements recorded by sensors were acquired, organized, and analyzed using R environment v.4.0.3 [44]. For quality control, we followed the methods developed by Serrano-Notivoli et al. (2017, 2019) [45,46] for fine-scale temperature datasets. A suspicious value was defined as: (i) a T_n higher than the T_x in the same day, (ii) five consecutive daily temperatures with the same value, or (iii) outliers. We did not interpret as suspicious those series of values between −1.5 and 1.5 °C recorded over weeks by sensors located in elevated areas as they can be covered by snow in winter. Daily validated T_n and T_x data were then averaged to a monthly scale when there was a minimum of 21 days per month with validated records.

Differences in the year of sensor installation, battery issues, and the loss of some of them through time resulted in temporal series of different lengths and introduced some gaps in the time series. To overcome this problem, reduce potential bias due to interannual variability with different numbers of years, and generate a stronger characterization of the sampled areas, we decided to build a “month/season/year-type” for T_n, T_x, and VPD_{max} for each site (i.e., mean T_n, T_x, and VPD_{max} values for each month, season, and year) (Table 1). The use of an average metric to characterize extreme values is supported by the recent work of Wolf et al. (2021) [18], who demonstrated the high year-to-year consistency of thermal characteristics of microrefugia across a mountain area. Thus, we generated season-type and year-type T_n and T_x metrics for both air and soil, averaging monthly data across seasons and years. We used the last three years (36 months) for each site for air T and all available monthly data for soil T with at least one complete year (>12 months). The total numbers of sites that fit those criteria were 76 and 54 for air and soil, respectively. Besides the monthly, seasonal, and yearly T_n and T_x, we selected the most extreme T_n and T_x monthly values for each site.

Table 1. Summary of microclimatic and refugial capacity metrics built for T_n, T_x, and VPD_{max}, based on a year-type (36 months for air metrics, and at least one year for soil metrics).

Metric	Description
Winter	Mean of December, January, and February
Spring	Mean of March, April, and May
Summer	Mean of June, July, and August
Autumn	Mean of September, October, and November
Mean Annual	Mean of the annual monthly values
Extreme Annual	Highest and lowest annual monthly values

Additionally, we derived two metrics related to the refugial capacity of each site: (i) the thermal amplitude (also named “stability”: ST), which serves to identify sites of low thermal range by the difference between T_x and T_n for each month, season, and year, and (ii) the buffering effect created by forcing-climate factors on T_n and T_x (also named “offsets”), which indicates how much the near-ground extreme T decouples from the air estimated one, as the difference between fine measurements estimated from iButtons (microclimate) and the ones provided by WorldClim (macroclimate).

2.4. Environmental Variables

To model microclimate T, we used a set of topographic and vegetation variables; the latter combined information about the intensity of vegetation and forest structure (Table 2). Topographic and forest structural variables came from public ALS-LiDAR data of the Spanish National Plan for Aerial Orthophotography project (PNOA), captured in 2010 for our study area. As National Parks are managed under very restrictive protection laws, the temporal lag between LiDAR acquisition and climatic estimations was considered appropriate as no significant changes took place in the PNOMP over that period. The sensor operated at a wavelength of 1064 μm and with a scan angle of ±29° from the nadir. We acquired 245 LiDAR files in “las” format, which were provided by the Spanish National Geographic Information Centre (IGN-CNIG) in 2 × 2 km tiles of raw data points. The average point cloud density was 1.5 point/m², and all returns had a vertical accuracy better than 0.2 m. The Geodetic reference system for x, y, and z coordinates was ETRS89 UTM 30N. The noise and overlap point classes were removed and ground points were classified according to Montealegre et al. (2015) [47], using the multiscale curvature classification algorithm implemented in the MCC-LiDAR v.2.1 command line tool [48]. These classified ground points allowed us to generate a digital terrain model (DTM) of 5 m spatial resolution using the LasTools module in ArcGIS v.10.7.1. We created the DTM for two main purposes: to derive a suite of topographic variables, and to normalize LiDAR heights in order to extract statistical metrics of the structure of vegetation and generate forestry variables.

Topographic variables, created at the same resolution as the DTM, were elevation (in m a.s.l.), slope (in degrees), northness and eastness (as the cosine and sine of aspect in radians, respectively), flow direction, heat load, and topographic position index (TPI). Slope, northness, and eastness were chosen for their large influence on microclimatic variability in roughness areas. Flow direction allowed for approximating the soil moisture content and modeling potential areas of water accumulation, acting as a proxy for the terrain wetness index. Heat load was created as a proxy of solar exposure or potential solar incoming radiation. TPI was used as a measure of terrain concavity and convexity and an approach to cold air drainage. Elevation data were extracted directly from the DTM. We used the “raster” package for the R environment [49] to generate the slope, northness, eastness, and flow direction. For the heat load and TPI, we used the “Terrain analysis” module implemented in SAGA-GIS [50].

Table 2. List of environmental variables selected to model microclimatic and refugial capacity metrics. T = Topographic variable; V = Vegetation variable.

Variable Name	Type	Min.–Max. Values	Description of Min./Max. Values
Elevation	T	587–3355 m a.s.l.	Lowest/Highest elevation
Slope	T	0–87.98°	Flat terrain/Maximum steep slope
Northness	T	–1–1	Southward/Northward aspect
Eastness	T	–1–1	Westward/Eastward aspect
Flow direction	T	1–128	Minimum/Maximum water accumulation
Heat load	T	–1–1	Minimum/Maximum solar exposure
TPI	T	–186–254	Concave/Convex landforms
NDVImax	V	0–1	No intensity/Maximum intensity of vegetation
Canopy closure	V	0–100%	0%/100% of sky covered by vegetation from a single ground point
Elev. CV	V	0–7.55	Minimum/Maximum variability of vegetation heights
Strata below 1 m	V	0–1	No returns/All returns proportion below 1 m

Because the forests of the PNOMP show a large variation in terms of dominant tree species and their development (tall trees in the lowest, soil-rich valleys, and small ones at the timberline), the vegetation structure is heterogeneous in height and canopy density. Therefore, several statistical metrics of vegetation structure were obtained using FUSION/LDV v.4.21 open source software [44]. We normalized the non-ground point cloud heights using the DTM previously created, and then we clipped the point cloud to each plot with a circular radius of 7.5 m from the sensor location. We extracted metrics related to the canopy height distribution (height percentiles: P01, P05 . . . P99), canopy height variability (standard deviation and coefficient of variation of heights), and canopy cover density (canopy closure and percentage of returns at different height strata: below 1 m, 1–2 m, 2–4 m, and above 4 m). To avoid incorrect estimates from the metrics, we used the Spanish National Forest Map (MFE50, https://www.miteco.gob.es/es/biodiversidad/servicios/banco-datos-naturaleza/informacion-disponible/mfe50_descargas_ccaa_aspx, accessed on 23 February 2022) as a mask to delimit ALS-LiDAR points that actually belong to vegetation. Subsequent statistical analyses (see below) allowed for the selection of three forestry variables: Canopy closure, Elev. CV, and Strata below 1 m. Canopy closure is defined as the proportion of the sky hemisphere covered by vegetation from a single ground point [51]. Elev. CV is the height coefficient of variation in the LiDAR point cloud, thus referring to the variability of vegetation in height. Strata below 1 m is the proportion of returns with respect to all returns located below 1 m, referring to the percentage of low vegetation strata (shrubs, bushes, grasses).

Finally, the vegetation intensity was generated through the calculation of the maximum value of the NDVI (Normalized Difference Vegetation Index). Data were obtained from a time-series of images with Landsat’s TM, ETM+, and OLI sensors between 2010 and 2020. Using Google Earth Engine (GEE), a series of corrections of surface reflectivity images were applied to this collection: cloud, shadow, snow, and water masks with the “CFmask” algorithm, Minnaert topographic correction using the USGS GMTED2010 digital elevation model, and harmonization of all the scenes of the collection to the OLI sensor of Landsat 8.

2.5. Statistical Modeling

Prior to statistical modeling of microclimatic metrics and the refugial capacity, we made a selection of structural explanatory variables from a long list produced by ALS-LiDAR statistical metrics. We checked for correlations among them to avoid collinearity and thus reduce the number of explanatory variables (Figure S1, Supplementary Material). Furthermore, we checked them for collinearity again using variance inflation factors (VIFs)

after modeling, from the “car” package in R [52]. To facilitate the interpretation of beta coefficients in model outputs, all variables were standardized to have the mean 0 and standard deviation 1.

A total of 66 microclimatic and refugial capacity metrics were used as dependent variables. Microclimatic metrics corresponded to the air (Tn, Tx, and VPDmax) and soil (Tn and Tx), the month of highest (Tx, VPDmax) or lowest (Tn) value (also named as “extreme annual”), the four seasons, and the mean annual (average of 12 months). The same scheme was used to calculate the refugial capacity metrics: ST (though in this case annual ST was calculated as the difference between the Tx of the warmest month and Tn of the coldest one) and offsets for Tn and Tx using WorldClim as a reference.

Generalized linear models (GLM) were built to assess the effect of each selected explanatory variable on microclimatic and refugial capacity metrics. For each response variable, we chose the model structure that minimized the AIC value using the “dredge” function in the “MuMin” package in R [53]. This method compares all possible combinations of variables and finds the most explanatory (but parsimonious) set based on the lowest AIC value. We also explored the effect of interaction terms between slope and aspect (northness and eastness), but they were never significant. The model performance was assessed using R^2 and the root mean square error (RMSE). The latter was calculated from models with non-standardized variables, so they refer to the °C and kPa error in T and VPDmax, respectively. The relative importance of each statistically significant variable in the model of lowest AIC was calculated using simple unweighted averages over orderings, using the package “relaimpo” in R [54], and rescaled to the R^2 of each model to compare their real importance.

3. Results

3.1. Climatic Diversity and Performance of Microclimatic Models

Our network of *iButtons* evidenced the existence of important climatic diversity over a small but topographically complex area. Figure 4 showcases such heterogeneity, not only because of the large differences between open areas and forests but also within those two types of environments. For example, beyond the classical idea of milder temperatures in forests than in open areas, or a narrower thermal range in the soil compared to air, we found that Tx can span a yearly range of between 14.4 °C (site “O22”) and 27.6 °C (site “A2”) in open areas, the vegetative period can span 4 to 12 months depending on the length of the period of snow cover (same sites as before), and forests can experience a Tn below 0 °C aboveground during wintertime (site “P7”).

Microclimatic models of fine-scale metrics (Tn, Tx, and VPDmax) and refugial models (ST and offsets of Tn and Tx) were all statistically significant ($p < 0.001$) and fit well for both the air and soil (Table 3). The model fit was slightly better for soil T ($R^2 = 0.43 - 0.93$) than air T ($R^2 = 0.34 - 0.87$) or VPDmax ($R^2 = 0.39 - 0.86$). Tn always fit better than Tx for both air and soil, except for in Winter and the Extreme Annual. The highest fit values were always reached in Spring for Tn, Tx, and VPDmax, while Extreme Annual had the lowest ones in all cases, especially in the air. Mean Annual Tn, Tx, and VPDmax also fit well, usually in second or third place among the six metrics for each combination of air/soil and Tn/Tx in which that particular metric was included. The RMSEs were lowest for soil Tn (0.81–1.29 °C), and highest for air Tx (2.05–3.82 °C). Regarding refugial metrics, the R^2 of ST ranged from 0.43 to 0.66, and although the R^2 was similar in air and soil (slightly higher in soil except for Spring and Mean Annual), the RMSE was lower in soil (0.68–2.59 °C) than air (2.29–3.91 °C). The R^2 of offset values ranged from 0.35 to 0.76 in air T, and 0.51 to 0.86 in soil T, and generally fit better for Tn than Tx. The lowest R^2 corresponded to Tn in Winter and Tx in Summer in the air, most likely due to the temperature uniformity created by snow in the former case and some overheating by solar radiation in the latter.

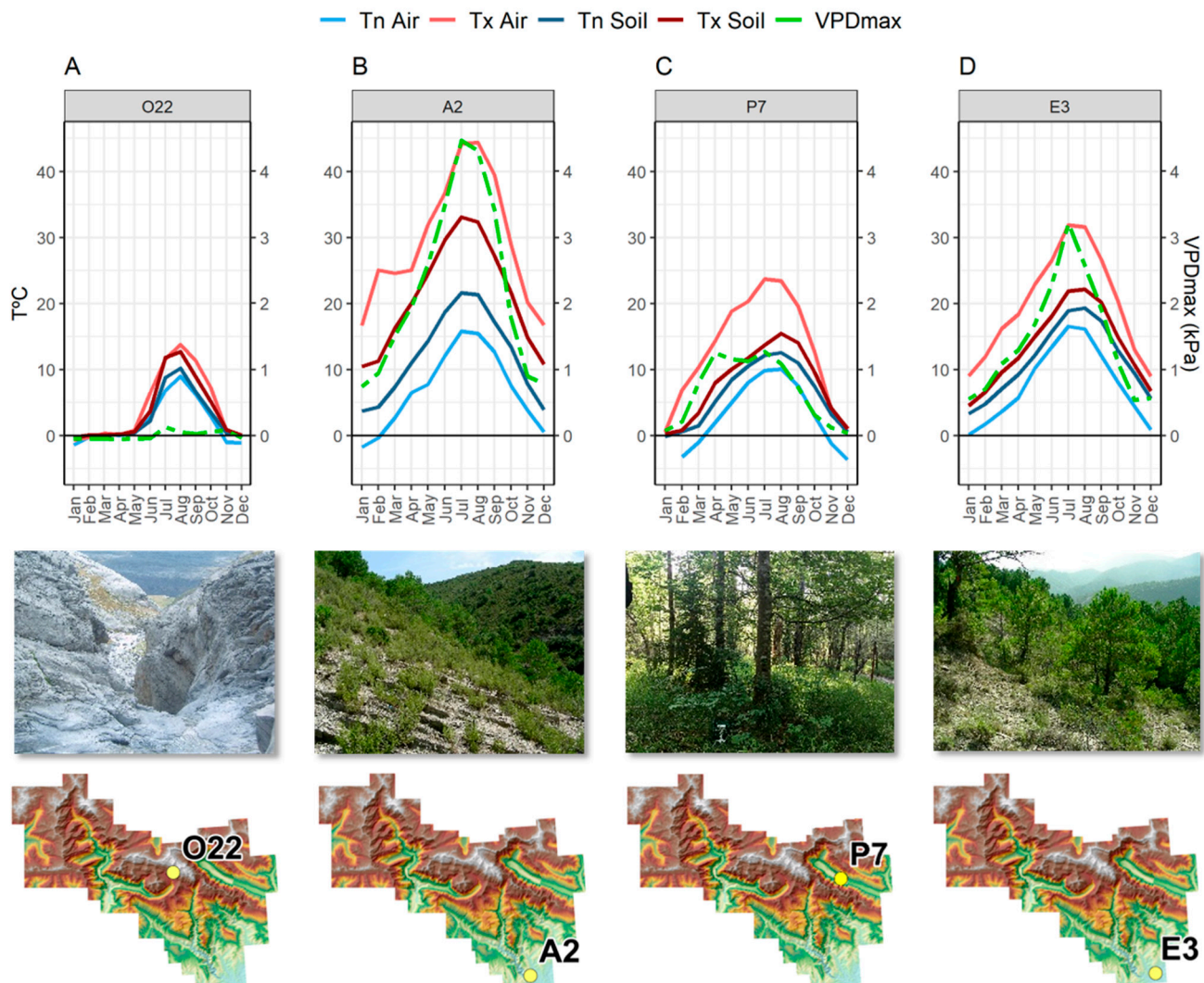


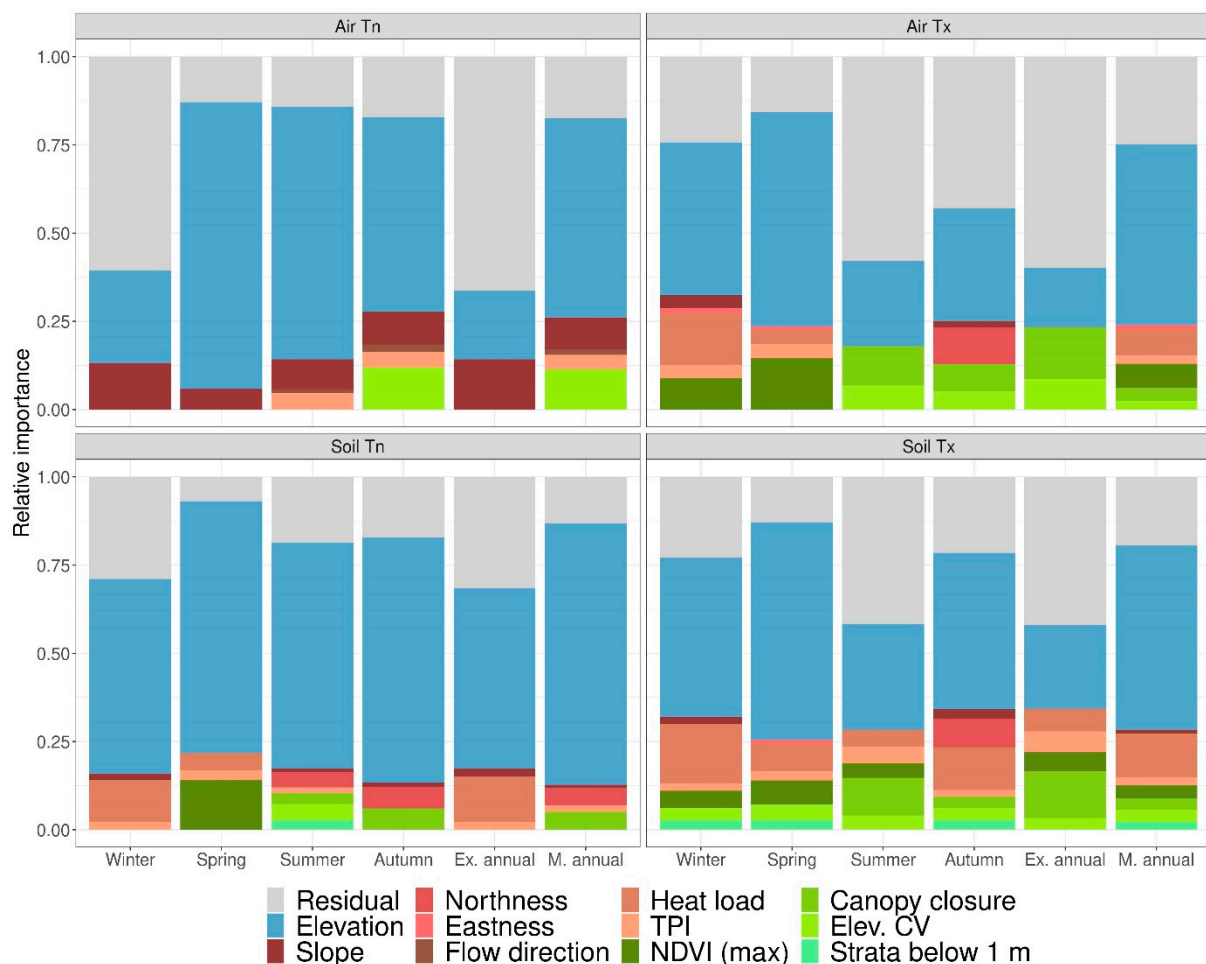
Figure 4. Monthly Tn and Tx in air and soil, and VPDmax, of four contrasted sites at the PNOMP, corresponding to the coldest (A–C) and warmest (B–D) sites in open (A,B) and forest (C,D) areas.

3.2. Variables behind Microclimatic Diversity (Tn, Tx, and VPDmax)

Microclimatic models included several topographic and vegetation variables (Table S1, Supplementary Material), except in the case of air Tn, which were basically fitted with the elevation and slope. The analysis of predictors' relative importance revealed that forest variables contributed more than topographic ones in Tx models, and also in Spring and Summer for soil Tn models (Figure 5). Elevation was the most consistent (significantly negative) predictor in all microclimatic Tn and Tx models, stronger for Tn than Tx, and for air than soil (Table S1, Supplementary Material). In fact, we found that when elevation had a poor relevance in models, the R^2 decreased. The TPI, slope, and heat load were also significant in several models and their relationships were positive in all cases. This means that temperatures tend to be warmer in steeper areas, especially in southern exposures, while cold air tends to flow into the valleys and concave reliefs. In addition, the TPI was significantly positive in all VPDmax and soil models (except for the Autumn soil Tn), indicating that there is less water deficit in concave landforms and valleys. Eastness was also a small but significant (positive) predictor of Tx. Regarding vegetation variables, canopy closure, Elev. CV, and NDVI always exerted a negative effect on Tx, both in the air and soil, while strata below 1 m was a frequent positive predictor of Tx. This means that the greater the presence of trees and other plants, the lower the Tx. Likewise, sites with abundant low strata (i.e., with an absence of trees) tended to be warmer.

Table 3. GLM model performance of microclimatic and refugial capacity metrics for T and VPD. All models were statistically significant (p -value < 0.001).

		Microclimatic Metrics				Refugial Capacity Metrics						
						Stability			Offsets			
		Air Tn	Air Tx	Soil Tn	Soil Tx	VPDmax	Air ST	Soil ST	Air Tn	Air Tx	Soil Tn	Soil Tx
Winter	R ²	0.39	0.76	0.71	0.77	0.64	0.62	0.66	0.76	0.49	0.86	0.76
	RMSE	1.46	2.06	0.96	1.21	0.12	2.29	0.68	1.25	2.03	0.75	1.14
Spring	R ²	0.87	0.84	0.93	0.87	0.86	0.62	0.51	0.72	0.41	0.51	0.56
	RMSE	0.84	2.31	0.81	1.46	0.16	2.68	1.13	0.72	2.43	0.77	1.51
Summer	R ²	0.86	0.42	0.81	0.58	0.49	0.38	0.43	0.35	0.36	0.62	0.58
	RMSE	1.20	3.55	1.29	2.46	0.53	3.91	2.03	1.09	3.61	1.06	2.42
Autumn	R ²	0.83	0.57	0.83	0.78	0.51	0.48	0.51	0.58	0.52	0.70	0.73
	RMSE	1.13	2.70	1.12	1.42	0.31	2.89	1.19	1.00	2.70	0.80	1.36
Mean Annual	R ²	0.83	0.75	0.87	0.81	0.63	0.48	0.47	0.69	0.45	0.76	0.68
	RMSE	1.01	2.05	0.92	1.37	0.23	2.43	1.13	0.87	2.19	0.68	1.40
Extreme Annual	R ²	0.34	0.40	0.68	0.58	0.39	0.43	0.52	0.40	0.41	0.73	0.61
	RMSE	1.63	3.82	0.91	2.51	0.70	3.91	2.59	1.19	3.83	1.05	2.56

**Figure 5.** Relative importance of explanatory variables for modeling Tn and Tx recorded by in situ sensors in the air and on the ground over the 2100 m altitude of the PNOMP. The columns correspond to one of the six models: the four seasons, the annual extreme (Ex. annual), and the annual mean (M. annual).

VPDmax was mainly influenced by elevation (Figure 6), especially in Winter and Spring: the higher the site, the lower the drying power of the air, most likely due to two

effects: the probability of being under snow and as VPDmax is lower for cold than warm T for the same relative humidity. Site exposure (TPI) was a consistently positive explanatory variable in all periods considered: the more exposed, the higher the VPDmax, followed by heat load and eastness. Variables related to the forest density or structure reduced the VPDmax but contributed less than to Tx models.

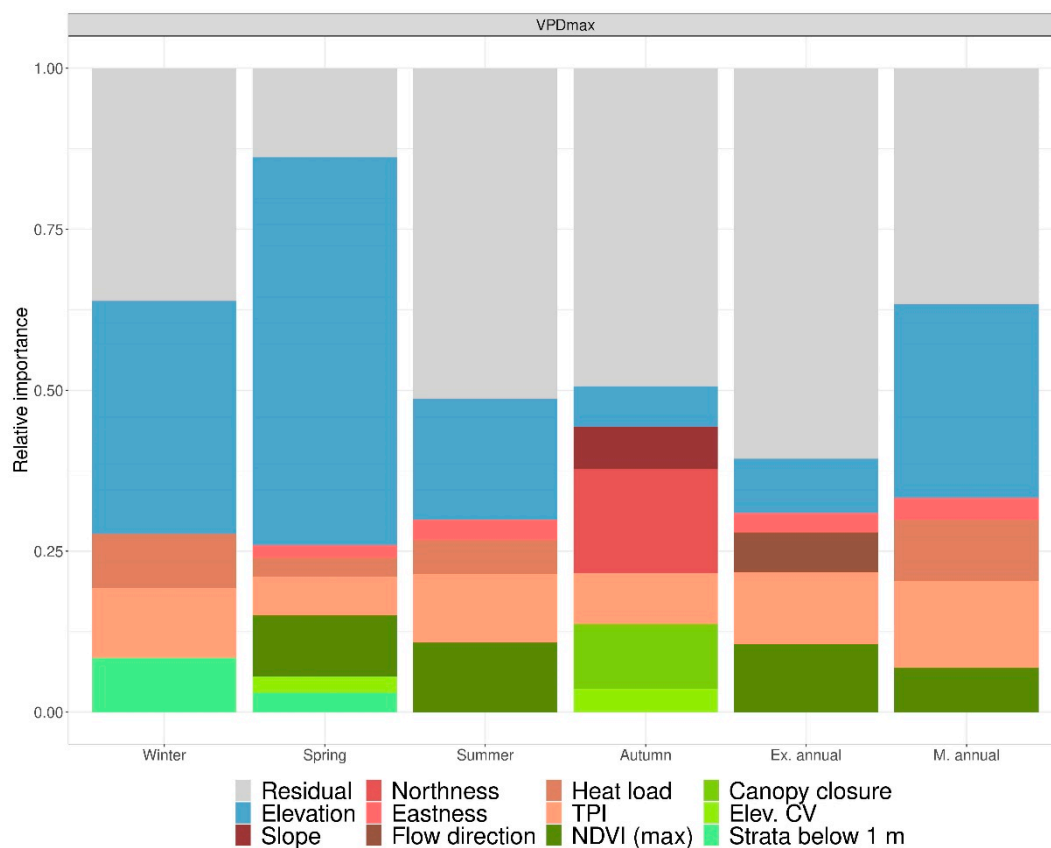


Figure 6. Relative importance of explanatory variables for modeling VPDmax from relative humidity and temperature recorded by in situ sensors in the air along 2100 m of elevation. The columns correspond to one of the six models: the four seasons, the annual extreme (Ex. annual), and the annual mean (M. annual).

3.3. Open Versus Forested Microclimates

As expected, the temperature in forests was milder than in open areas across the year, the pattern being clearer for Tx than Tn (Figure 7). This agrees with microclimatic models as forest predictors had strong significance in Tx. While Tn was higher in forests compared to open areas, especially for the air in Spring and Summer, Tx was markedly lower in forests in Summer and Autumn, especially in the air. Tx showed a very large variability across sites in Winter and Spring, most likely due to the variability of snow presence. VPDmax showed higher values in forests during Winter and Spring (probably due to the variability in the presence of snow across sites) and lower afterward, indicating the beneficial effect of the canopy in lowering the VPDmax during the warmest period (Figure 8).

3.4. Factors Promoting Refugial Capacity

Thermal stability (ST) was narrower in soil than air due to the higher Tn and lower Tx in soil (Figure 9). Models revealed that elevation was only relevant as a negative predictor of ST (increases ST) in Winter and Spring, while it was not even significant for the soil in Summer (Table S2, Supplementary Material), most probably because soils can warm considerably at any elevation in the warmest period. As an example, the soil of a subalpine grassland looking slightly southwest at 2450 m high can warm up till reaching a monthly

Tx of 22 °C in July (Figure 9A). Interestingly, we found a very good association between the Tx of the warmest month and the thermal annual range (Figure 9), both in open ($R^2 = 0.93$ after pooling air and soil data) and forested sites ($R^2 = 0.86$). This means that the cooler sites become in Summer, the more thermally stable they are throughout the year.

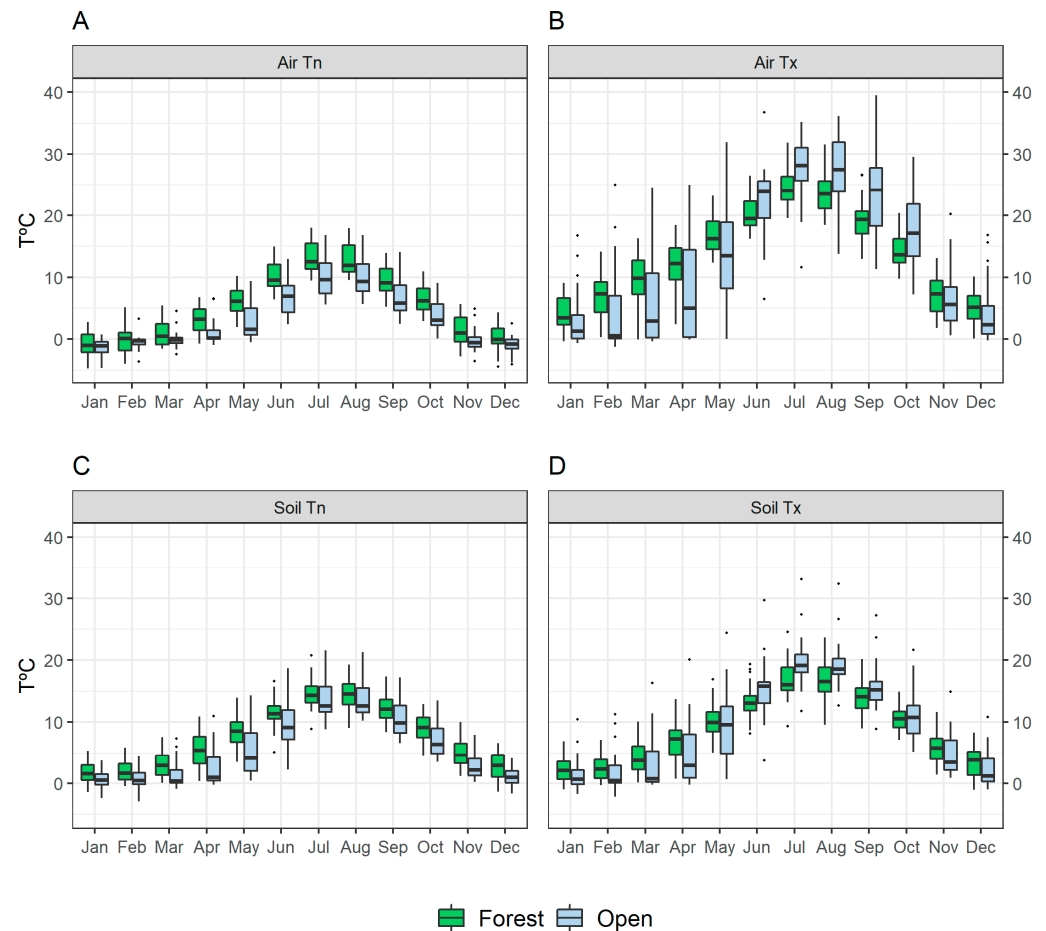


Figure 7. Boxplots to compare daily Tn and Tx in open and forested habitats over a full year-type in the PNOMP, both in the air (A,B) and soil (C,D).

The contribution of elevation to ST, however, was minor compared to microclimatic models (Figure 5), and much lower than vegetation variables in the warm photosynthetic period (Figure 10). Among topographic variables, the eastness, TPI, and heat load were also often relevant for ST, always in a positive way, meaning that less thermally stable areas are located in less northern exposures and concave reliefs (valleys). Vegetation variables were always highly relevant for thermal stability and contributed to all ST models (Figure 10 and Table S2, Supplementary Material): NDVI, canopy closure, and Elev. CV negatively, and strata below 1 m positively. These four variables influence ST in the same way as in microclimatic models: the higher the intensity of vegetation, canopy height variability, and canopy density, the higher the ST, whereas the presence of low strata (herbs and bushes) is associated with open sites and lower ST. As a consequence, thermal stability is higher and more homogeneous throughout the year in forests than in open areas, both in air and soil (Figure 11). The greatest contrast of thermal ranges in forests compared to open areas is achieved in Summer, both in air and soil. On the other hand, the huge variability found among open areas is most likely due to the fact that (sub)alpine grasslands can be “protected” at 0 °C under snow for months, whereas the sun heats the lowest and warmest open sites early in spring.

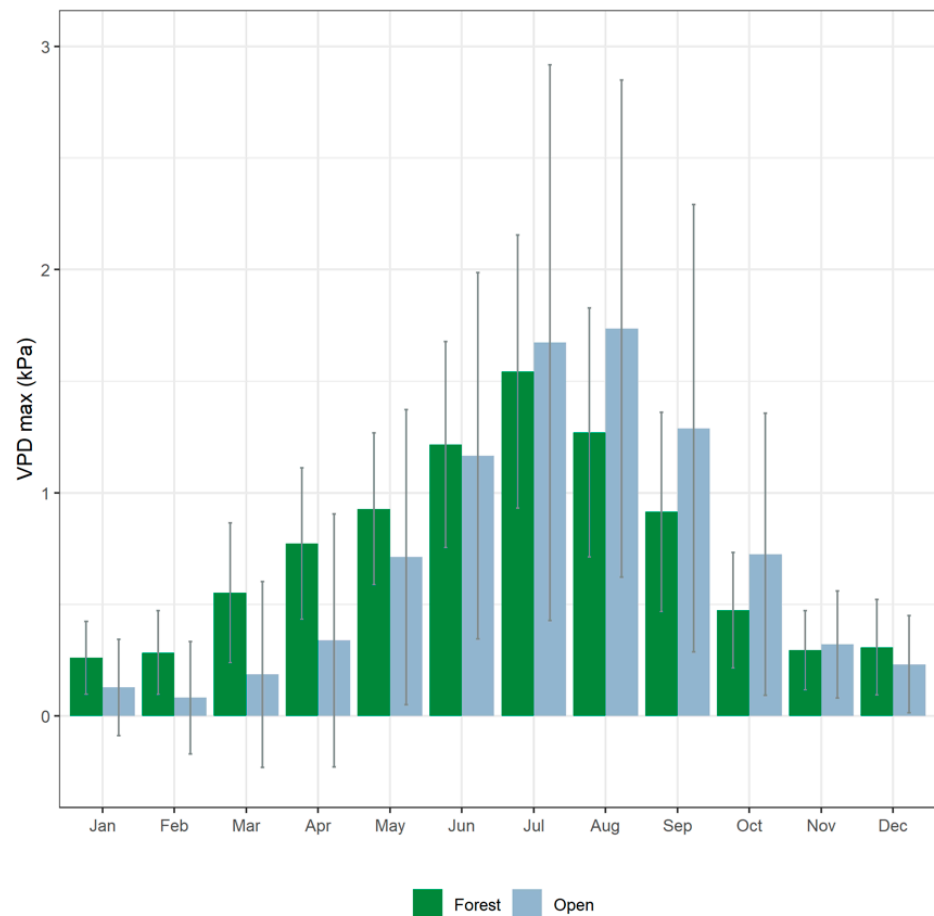


Figure 8. Histogram to compare the mean + SD of VPDmax in open and forested habitats of the PNOMP over a full year-type (see further details in text).

Since offsets are calculated as the difference of micro-macro T , estimated from in situ sensors and WorldClim, respectively, they are recognized as such by means of negative values for T_x and positive values for T_n . Elevation was no longer consistently significant: it positively affected the T_n offset in the air all the way throughout the year, and the soil in Winter and Autumn (most likely due to the snow cover effect), while it negatively affected T_x in Spring (meaning that decoupling is lower in the upper part, likely due to the protective effect of snow) (Table S2, Supplementary Material). Northness contributed considerably to many offset models, especially for soil T_n , always negatively, and therefore, it can be considered an important variable for offsetting high temperatures. Elev. CV was a very frequent and important contributor to offset models, similar to NDVI and canopy closure. In T_x offset models, canopy closure made a large (negative) contribution for Summer and Extreme Annual in the air and soil, although other forest variables contributed equally or more in the soil (Figure 12). This means that: (1) forests significantly decouple the warmest temperatures of the year, (2) the higher the forest density, the higher the offset of T_x , and that (3) not only canopy but also the presence of vegetation in general has a stronger effect than topographic variables during the warmest season or month. T_n offset models showed a more balanced and complex contribution of variables: a lower contribution of forest structure and higher effect of other topographic variables such as slope and northness. NDVI entered as a relevant predictor for most metrics and periods of soil offset models, along with Elev. CV, canopy closure, and strata below 1 m.

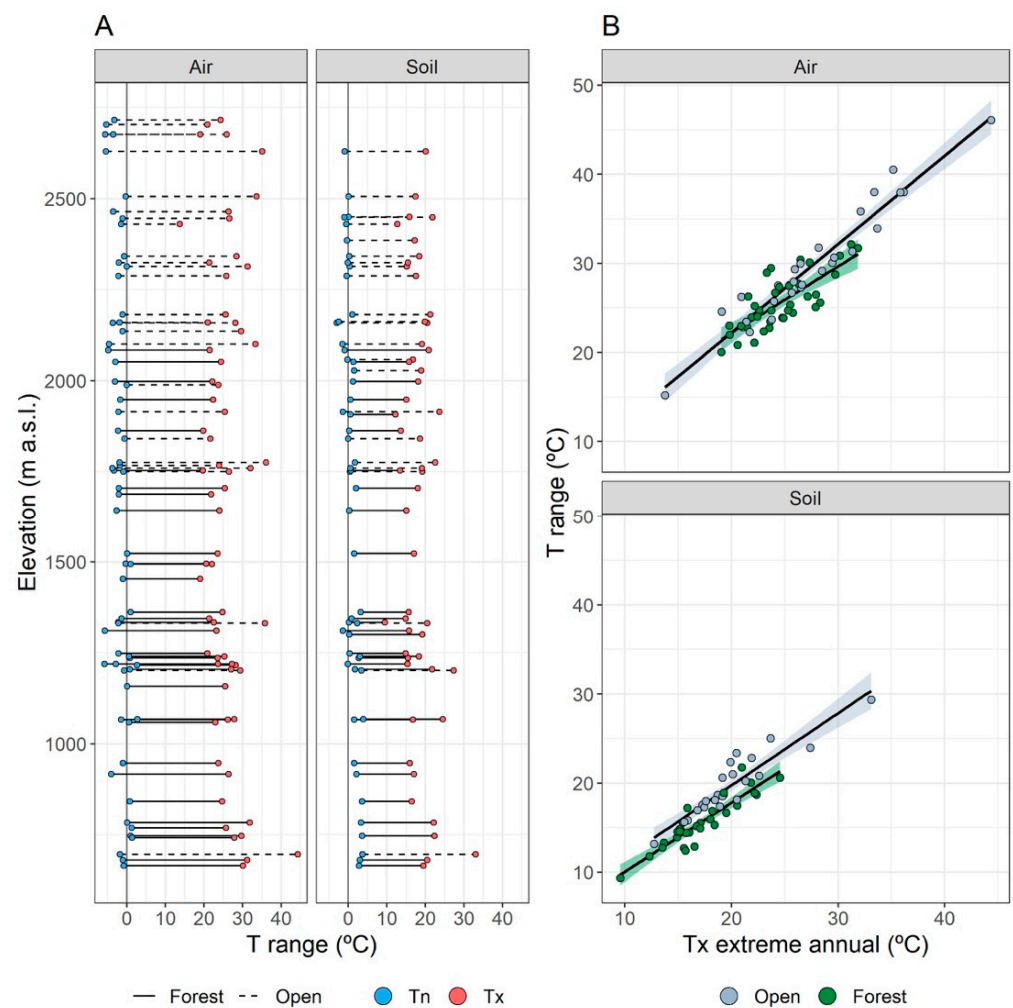


Figure 9. (A): Thermal range in air and soil (stability: Tx of the warmest month, Tn of the coldest one) of monitored sites in the PNOMP across the elevation gradient of 2100 m. (B): Association between Tx of the warmest month and the thermal amplitude for open and forested habitats, for the air and soil.

As with thermal stability, we found that there was a greater offset of T in soils of forests than open areas (Figure 13). Forest variables had a substantial effect on soil Tx, especially between June and September, where the difference from the macroclimatic model exceeded 5 °C (with a maximum decoupling of 7.1 °C in August at one of the monitored sites). For soil Tn, forested areas had a more homogeneous decoupling throughout the year (between 3.8 °C and 5.4 °C). Decoupling of Tx in open areas was much lower (between 1.2 °C and 2.1 °C) and restricted to Spring and Summer, whereas the effect was much stronger for Tn (between 4.8 °C and 7.5 °C). This means that soils of open areas have warmer Tn than macroclimatic estimates but have similar Tx, and therefore, they show larger thermal ranges than forests throughout the year.

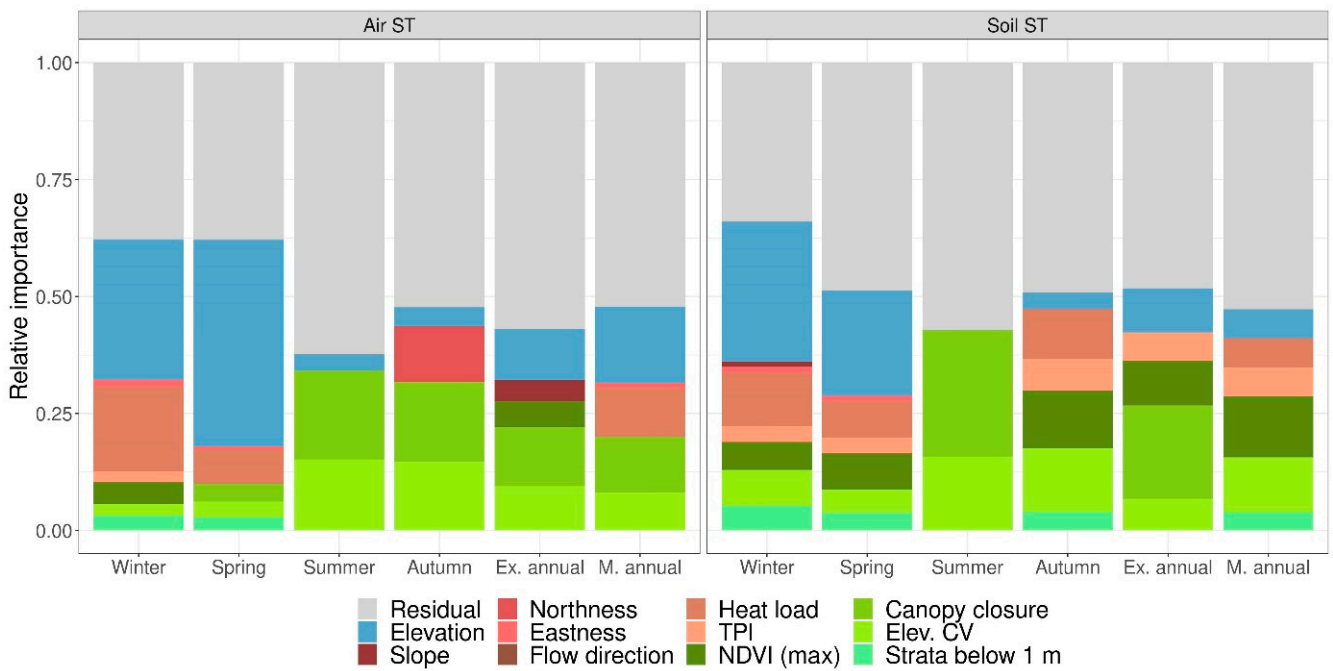


Figure 10. Relative importance of explanatory variables for modeling stability (Tx-Tn) from records taken by in situ sensors in the air and on the ground over the 2100 m altitude of the PNOMP. The columns correspond to one of the six models: the four seasons, the annual extreme (Ex. annual: Tx of the hottest month, Tn of the coldest month), and the annual mean (M. annual: average of the 12 monthly stabilities).

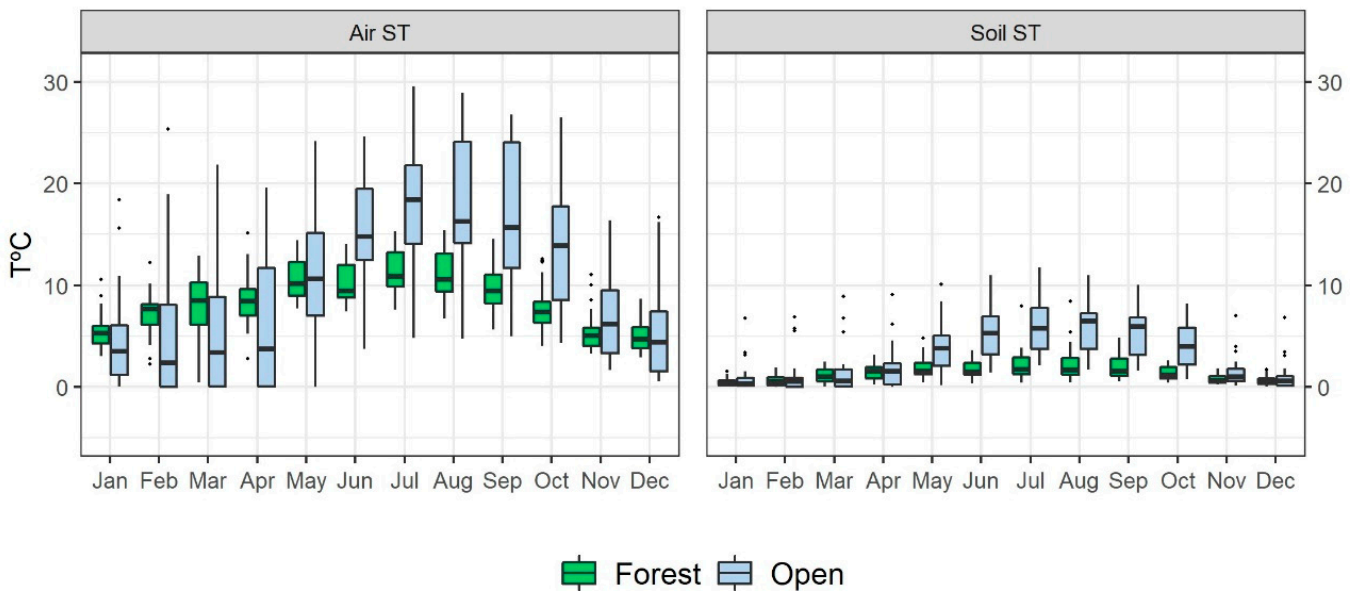


Figure 11. Boxplots to compare thermal stability in open and forested habitats over a full year-type in the PNOMP, both in the air and soil.

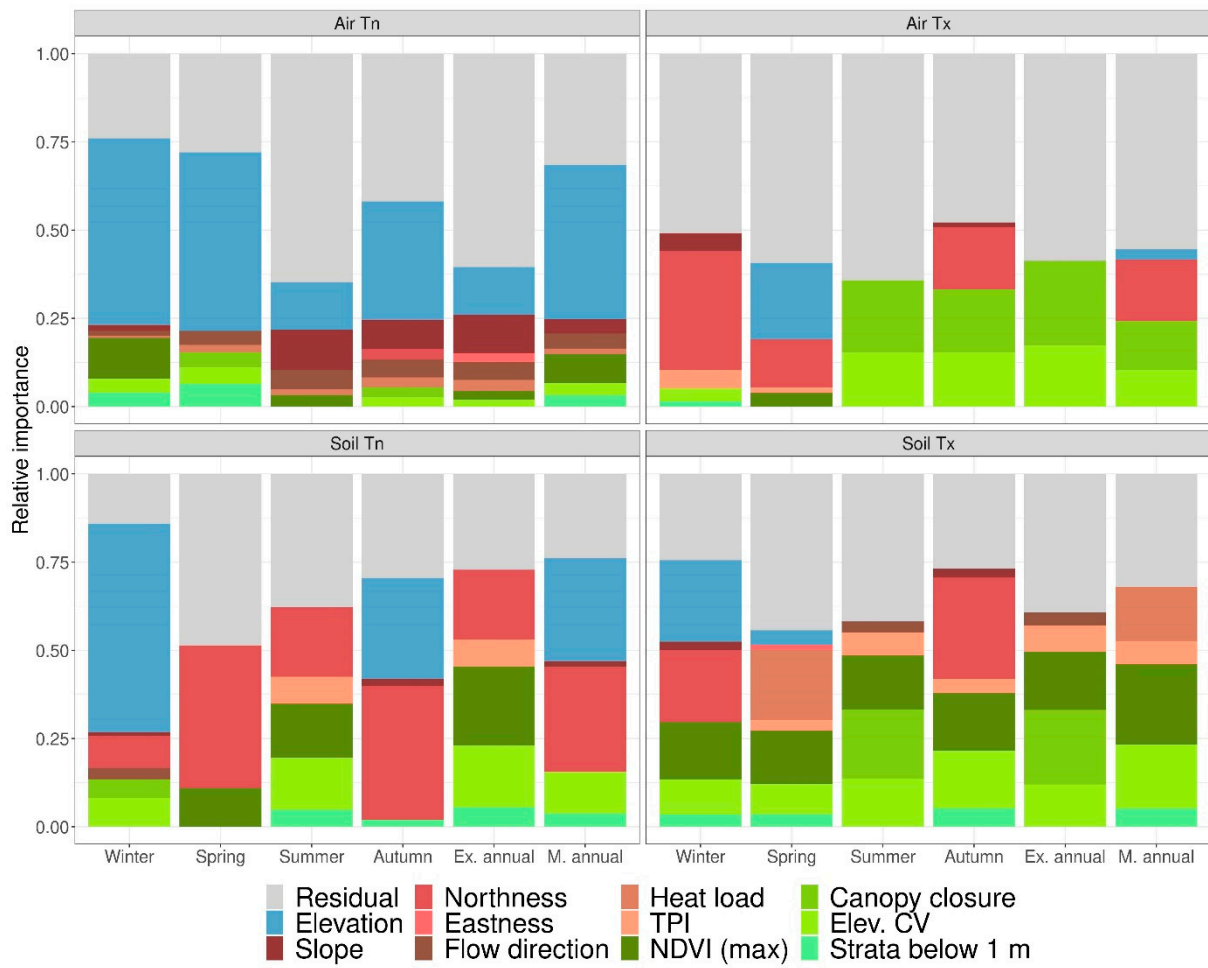


Figure 12. Relative importance of explanatory variables for modeling T offsets (T recorded by in situ sensors, T estimated by WorldClim) in the air and soil along 2100 m of the elevation of the PNOMP. The columns correspond to one of the six models: the four seasons, the annual extreme (Ex. annual), and the annual mean (M. annual).

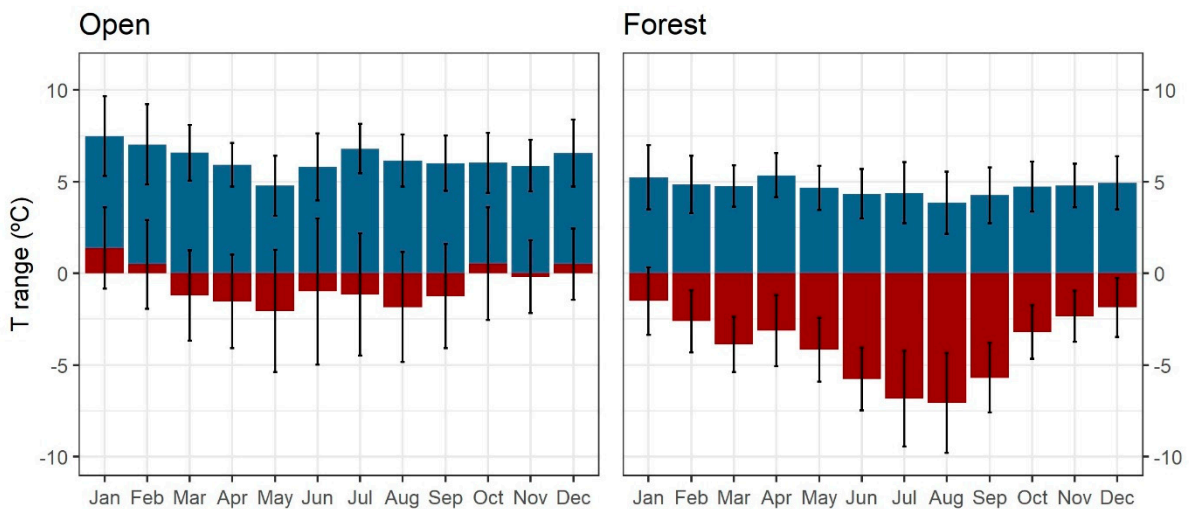


Figure 13. Monthly offsets of Tn (in blue) and Tx (in red) in the soil of open and forested habitats along 2100 m of the elevation of the PNOMP. Offsets were calculated as the difference between micro- and macro-temperatures, as recorded by in situ sensors and estimated by WorldClim, respectively.

4. Discussion

Our study has revealed the large variety of microclimates held in a small but environmentally heterogeneous mountain area of southern Europe, and the poor fit with a frequently used macroclimatic model (WorldClim). We modeled extreme temperatures (Tn, Tx), the vapor pressure deficit (VPDmax), and refugial capacity (stability and offset from regional climate) over a year-type, and disentangled the role of several topographic and vegetation variables acquired through LiDAR and optical imagery (Landsat). Overall, the results highlighted the importance of vegetation in general, and forests in particular, in narrowing thermal ranges and offsetting extreme temperatures at a local scale. They also demonstrated that temperature records above- and below-ground do not match and are not interchangeable, which should be taken into account when describing the thermal niche of organisms.

4.1. Climatic Diversification: Beyond the Effect of Elevation

Microclimatic models performed well enough to adjust fine-scale measurements recorded by the network of miniaturized sensors over an important elevation gradient and a large variety of habitats, working better in soil than in air, and for Tn than for Tx. Although our study is based on a high density of iButtons (e.g., see for example [17,28,55]), we are aware that the microclimatic variability described is only a small sample of a very climatically diversified landscape, as we did not deploy any sensor in the many small-sized geomorphological niches, some of them identified as refugia for boreoalpine and cold-adapted relict species [12,13].

Similar to previous studies of microclimates in mountains of contrasted bioclimatic areas like the southeast of Australia [56], Scandinavia [57], and the Mediterranean Alps [58], our results show that heterogeneous terrains promote strong climate diversification beyond the dominance imposed by elevation, the classical explanatory variable of macroclimatic models based on meteorological stations. Since the elevation range in our study site is very large, elevation was expected to play an important role in determining extreme temperatures across the mountain landscape. That was the case, and we found that its importance was higher for Tn than Tx (see also [59]), and in soil than in air. In fact, elevation was less important in predicting Tx variability in the warm season, the most stressful and intensive period of vegetative growth. Interestingly, the poor relevance of elevation in microclimatic models coincided with a lower model fit and the appearance of other topographic and forest explanatory variables in the models.

Taking advantage of remote-sensing technologies capable of quantifying at very precise resolutions the intensity of vegetation (NDVI) and the structural complexity of forests at the ground-atmosphere boundary (ALS-LiDAR metrics: canopy closure, Elev. CV, and strata below 1 m), we could unveil which topographic and vegetation forcing-factors affected microclimatic metrics, and their relative contributions. Topographic variables exerted a higher effect on above-ground Tn and vegetation variables on Tx, whereas both kinds of variables exerted more balanced effects below-ground. The VPDmax was less affected by elevation except for in Spring, for which topographic variables contributed slightly more than vegetation ones (see also [38]). The importance of being able to maintain a low VPDmax lies in how sites that stay moister are better buffered from temperature fluctuations: Ashcroft and Gollan (2012) [56] showed that the diurnal range of both soil and air temperatures was reduced under moist conditions, whereas it increased under drier conditions. Consequently, sites of high resilience to climate change would be located in sheltered gorges, forests, and at high-elevation sites, even if they are not necessarily the places that experience the coolest temperatures [56].

Although previous studies modeling microclimatic diversity over large areas might have used a different set of explanatory variables, theirs and ours basically coincide in that slope and aspect (in our case, slope, northness, and heat load) influence radiation, and wind exposure (TPI) has a larger relative influence on the atmospheric water balance. Physiographic factors have often been acknowledged to mediate temperature and moisture, and

they are key to building topoclimatic models [12] and identifying microclimatic refugia [10]. However, although topoclimatic models considerably improve conventional approaches based on coarse grids and classical meteorological stations, they still do not account for the canopy cover [60,61]. Forest canopies strongly buffer extremes not only in Tx but also VPD throughout the growing season [30]. Each layer of vegetation, from the tree canopy to ground-level grass, constitutes an insulating factor that affects incoming radiation. Our analysis demonstrated that the presence of a horizontal (NDVI) and vertical (ALS-LiDAR metrics) vegetation structure drives microclimatic near-ground conditions and determines underground temperature heterogeneity as much as in the air. As a result, open lands and forest interiors showed important differences in the variability of microclimatic metrics. Our open habitats included a large variety of landscapes in terms of elevation, topography (slope and exposure to winds and solar radiation), and vegetation (from Mediterranean shrublands to dense subalpine grasslands and almost bare screes). The large variability of topographic variables and vegetation cover in open habitats is likely behind the higher variability of climatic metrics compared to wooded sites, as found by Gunton et al. (2015) [55] over a more extensive area.

4.2. Refugial Capacity

Climatic diversity underpins climate microrefugia. Here, we explored two factors related to refugial capacity: stability (ST) and offset. To some extent, they are linked, but we analyzed them separately for two reasons: (i) the former informed on factors promoting narrow thermal ranges irrespective of where they are in the “cold-warm” continuum, whereas the latter focused on the mechanistic decoupling of local Tn and Tx from the corresponding regional figures (from WorldClim in our case), and quantified the positive or negative offset of each metric. (ii) While ST is calculated as the difference between metrics taken by our own equipment, offset uses estimations provided by the global coarse-scale climate layer of WorldClim as a baseline [62], whose spatial resolution is much coarser than our microclimatic measurements, and therefore, a higher degree of uncertainty is expected for this metric compared with ST.

Instead of estimating ST in a dynamic way by comparing the present conditions with uncertain predictions of the future climate (see, for example, [63]), our metric focused on the actual thermal range of local sites. We found that the ST of T was hardly driven by elevation, except in Winter and Spring, most likely due to the protective effect of snow cover high in the upper part. Other factors related to the exposure to solar radiation (heat load), TPI, NDVI, and forest structure drove ST in the most intensive photosynthetic period and over the whole year (extreme annual) in the air, whereas little beyond the canopy closure contributed to explaining the ST in soil. The interpretation of the role of ST in the context of future biodiversity conservation needs to be qualified because the refugial role of current thermally stable places will depend on the type of variables behind it. If they are topographic ones, we can be confident in their long-term refugial role. For example, García et al. (2020) [35] showed that unvegetated cliffs acted as refugia for two relict plant species in the Pyrenees because those cliffs were thermally more stable than surrounding vegetated areas. Maclean et al. (2015) [22] empirically demonstrated that plant communities were more stable and less responsive to climate change on cooler slopes because those were the places where the extinction of species with low temperature requirements was delayed. We also found a highly positive relationship between Tx and the thermal range, evidencing that the coolest places are also the most stable ones. Although future climate change exposure has been found to be very large at high elevations, topographic buffering on poleward-facing slopes can moderate it [63]. The future refugial role, however, could decrease or disappear depending on the snow cover or other variables sensitive to global warming, and no mitigating action will likely be able to revert the situation. Given the role of vegetation in determining ST, the refugial capacity might change as a consequence of the indirect effect of climate change on vegetation, but forests can be managed to achieve the necessary conditions to sustain the refugial capacity. In summary, when mapping climate

stability, we need to qualify causal factors and how perdurable or manageable they are in the long term.

Offsets constitute one of the mechanistic tools promoting ST and the existence of climate microrefugia. Thermal buffering can dampen daily fluctuations, lessen the impacts of extreme temperatures such as regional heat waves and cold snaps, and moderate the general long-term increases in temperatures from climate change, resulting in greater overall thermal stability [64]. Our study revealed that decoupling between local microclimate metrics and WorldClim is mediated by topographic factors, the intensity of vegetation (NDVI), and forest structure (ALS-LiDAR metrics), which reversed or halted the dominant effect of elevation on extreme temperatures, both in the air and soil. LiDAR technology has been used to identify putative drought refugia from structural vegetation types in Australian granite outcrops [65]. Moreover, structural factors like the forest basal area were associated with the existence of microrefugia for plant species at their southern limit in boreal forests, particularly during the warm season [66].

Forests have received much attention in the last decade for their role as climatic refugia [62]: a comprehensive retrospective study covering thousands of stands of European forests demonstrated that recent changes to understory plant communities were more associated with changes to sub-canopy microclimates resulting from canopy cover dynamics than to regional climate change [67]. In addition, extremely hot temperatures under forest canopies are predicted to rise less than outside forests as the macroclimate warms up [68]. Thanks to the protective effect of the canopy, forests provide moderate conditions in terms of temperature and humidity compared to open lands, and this buffering promotes microclimates that function as microrefugia [30]. Nevertheless, the forest effect does not preclude additional effects of other factors, like the aspect in our case. Rita et al. (2021) [15] investigated the pattern of decoupling of the below-canopy temperature versus open-field, and demonstrated that, compared to the south-facing slope, the northern site exhibited less decoupling from free-air environment conditions and low variability in microclimate trends.

Some studies have also suggested that not all forests provide the same buffering. For example, old-growth forests with taller canopies, higher biomass, and more complex vertical structures, in particular, are the ones to reduce Tx temperatures and increase temperature stability [59,69]. We did not account for the age of forest stands, and trees have not been logged for at least 100 years in the PNOMP. Likewise, a threshold in canopy cover has been proposed, below which buffering properties in temperate forests largely would decrease [30,70]. In this context, Boehnke et al. (2021) [14] carried out a detailed study within a flat coniferous forest and demonstrated that the cooling effect of canopy shading resulted in comparably cool conditions in the forest soil and at the surface only in highly shaded sites, while the surface temperature reached considerably higher temperatures than nearby areas outside. Our study demonstrated that not only was canopy closure relevant for the refugial capacity but also the variability of tree heights (Elev. CV), the absence of high strata (strata below 1 m), and NDVI, emphasizing the importance of heterogeneity in the forest structure, besides the general presence of vegetation. Clearly, the physical process of buffering temperatures must reach a minimum intensity or structure to be fully operative. Nevertheless, some kinds of forests, such as those thriving under harsh conditions of the tree line, cannot become dense and yet still play an important role for species withstanding below or close to them. From the point of view of maximizing biodiversity conservation, very closed forests may not be the best situation as many species need a minimum of light to thrive. Mature forests with gaps could offer a better scenario, favoring the co-occurrence of organisms with different thermal profiles at short distances. Heterogeneous landscapes enlarge the range of resources and microclimates offered to organisms, which can buffer populations against climatic variation and generate more stable population dynamics [71,72].

5. Conclusions

In the current climate change context, identifying areas of high climatic diversity and those that will suffer the least from contemporary climate change (microrefugia) is the first step toward proactive and effective management to slow or halt biodiversity loss. With the help of miniaturized field sensors and active (LiDAR) and passive (Landsat) remote-sensing technologies, our study has demonstrated the important role of topographic and vegetation variables at a small scale to generate microclimate diversity and refuge capacity. Vegetation variables made a stronger contribution compared to topographic ones in lowering extremely warm temperatures, highlighting the key role of mountain forests in mitigating the expected increase in frequency due to climate change. Their sheltering capacity and manageability may make them the most important pieces for preserving biodiversity in a warmer world.

Species survival in microrefugia constitutes a mechanism for increasing resilience to climate change. However, the refugial concept is species-specific [73], and not all types of organisms can find refugia under the intense shade of the canopy. Integrative management to maximize biodiversity persistence would consist of protecting heterogeneous forests in terms of spatially varying solar radiation input, and also open areas where terrain-forcing factors can buffer the regional climate and reduce high levels of air drought. As stated by Morelli et al. (2020) [26], an effective climate adaptation strategy should encompass targets that are spatially diverse, temporally dynamic, and multifaceted. Remote-sensing can provide essential tools to detect areas that extensively accumulate different factors promoting refugial capacity, which should be prioritized based on their high resilience. We, therefore, advocate for the use of those technologies in conservation planning, given they can successfully identify at a small scale which places show the highest capacity to cope with or mitigate the effects of global warming, thus contributing to making mountains more resilient in climate-warming scenarios.

Supplementary Materials: The following supporting information can be downloaded at: <https://www.mdpi.com/article/10.3390/rs14071708/s1>, Figure S1. Correlations between environmental variables used for microclimatic models; Table S1: Significant variables of GLMs for the microclimate; Table S2: Significant variables of GLMs for the refugial capacity.

Author Contributions: Conceptualization, M.B.G.; data curation, R.H. and P.T.; formal analysis, R.H., H.M. and M.B.G.; methodology, R.H., H.M., M.P., M.B.G. and P.T.; resources, M.B.G.; software, R.H.; supervision, M.B.G.; writing—original draft, M.B.G.; writing—review and editing, R.H. and M.B.G. All authors have read and agreed to the published version of the manuscript.

Funding: This research was funded by the Autonomous National Park Organism, through the DYNBIO project (OAPN, 1656/2015); the Spanish Research Agency, through the VULBIMON project (CGL2017-90040-R); the European Commission, through the RESECOM project (LIFE+12 NAT/ES/000180) and the eLTER plus project (INFRAIA-01-2018-2019); the Spanish National Research Council (CSIC), through a JAE-INTRO fellowship granted to R.H. (JAEINT_18_01546), and the Government of Spain's Ministry of Science and Innovation, through an FPI predoctoral contract granted to H.M. (PRE2018-083868).

Institutional Review Board Statement: Not applicable.

Informed Consent Statement: Not applicable.

Data Availability Statement: Datasets are available on request.

Acknowledgments: Many people supported and/or helped with the deployment of miniaturized sensors. We thank the staff of PNOMP for facilitating this study in the protected area, and specially to the rangers that downloaded iButtons over the years: Carlos Benedé, Javier Gómez, Manuel Grasa, Rafael Jiménez, and Bosco Ponz. We also thank Patricia Abadía and Tom-Hadrian Sy for their help with data management, Miguel Ángel Saz and Roberto Serrano for their advice on climatic quality controls, and José Lahoz for reviewing the English text.

Conflicts of Interest: The authors declare no conflict of interest.

References

- Peñuelas, J.; Sardans, J.; Estiarte, M.; Ogaya, R.; Carnicer, J.; Coll, M.; Barbeta, A.; Rivas-Ubach, A.; Llusà, J.; Garbulsky, M.; et al. Evidence of Current Impact of Climate Change on Life: A Walk from Genes to the Biosphere. *Glob. Chang. Biol.* **2013**, *19*, 2303–2338. [[CrossRef](#)] [[PubMed](#)]
- Scheffers, B.R.; Meester, L.D.; Bridge, T.C.L.; Hoffmann, A.A.; Pandolfi, J.M.; Corlett, R.T.; Butchart, S.H.M.; Pearce-Kelly, P.; Kovacs, K.M.; Dudgeon, D.; et al. The Broad Footprint of Climate Change from Genes to Biomes to People. *Science* **2016**, *354*, aaf7671. [[CrossRef](#)] [[PubMed](#)]
- Gottfried, M.; Pauli, H.; Futschik, A.; Akhalkatsi, M.; Barančok, P.; Alonso, J.L.B.; Coldea, G.; Dick, J.; Erschbamer, B.; Calzado, M.R.F.; et al. Continent-Wide Response of Mountain Vegetation to Climate Change. *Nat. Clim. Chang.* **2012**, *2*, 111–115. [[CrossRef](#)]
- Dullinger, S.; Gattringer, A.; Thuiller, W.; Moser, D.; Zimmermann, N.E.; Guisan, A.; Willner, W.; Plutzer, C.; Leitner, M.; Mang, T.; et al. Extinction Debt of High-Mountain Plants under Twenty-First-Century Climate Change. *Nat. Clim. Chang.* **2012**, *2*, 619–622. [[CrossRef](#)]
- Loarie, S.R.; Duffy, P.B.; Hamilton, H.; Asner, G.P.; Field, C.B.; Ackerly, D.D. The Velocity of Climate Change. *Nature* **2009**, *462*, 1052–1055. [[CrossRef](#)]
- Sandel, B.; Arge, L.; Dalsgaard, B.; Davies, R.G.; Gaston, K.J.; Sutherland, W.J.; Svenning, J.C. The Influence of Late Quaternary Climate-Change Velocity on Species Endemism. *Science* **2011**, *334*, 660–664. [[CrossRef](#)]
- Scherrer, D.; Körner, C. Infra-red Thermometry of Alpine Landscapes Challenges Climatic Warming Projections. *Glob. Ecol. Biogeogr.* **2010**, *16*, 2602–2613. [[CrossRef](#)]
- Scherrer, D.; Körner, C. Topographically Controlled Thermal-Habitat Differentiation Buffers Alpine Plant Diversity against Climate Warming. *J. Biogeogr.* **2011**, *38*, 406–416. [[CrossRef](#)]
- Suggitt, A.J.; Wilson, R.J.; Isaac, N.J.B.; Beale, C.M.; Auffret, A.G.; August, T.; Bennie, J.J.; Crick, H.Q.P.; Duffield, S.; Fox, R.; et al. Extinction Risk from Climate Change Is Reduced by Microclimatic Buffering. *Nat. Clim. Chang.* **2018**, *8*, 713–717. [[CrossRef](#)]
- Dobrowski, S.Z. A Climatic Basis for Microrefugia: The Influence of Terrain on Climate. *Glob. Chang. Biol.* **2011**, *17*, 1022–1035. [[CrossRef](#)]
- Ashcroft, M.B. Identifying Refugia from Climate Change. *J. Biogeogr.* **2010**, *37*, 1407–1413. [[CrossRef](#)]
- Gentili, R.; Baroni, C.; Caccianiga, M.; Armiraglio, S.; Ghiani, A.; Citterio, S. Potential Warm-Stage Microrefugia for Alpine Plants: Feedback between Geomorphological and Biological Processes. *Ecol. Complex.* **2015**, *21*, 87–99. [[CrossRef](#)]
- Brighenti, S.; Hotaling, S.; Finn, D.S.; Fountain, A.G.; Hayashi, M.; Herbst, D.; Saros, J.E.; Tronstad, L.M.; Millar, C.I. Rock Glaciers and Related Cold Rocky Landforms: Overlooked Climate Refugia for Mountain Biodiversity. *Glob. Chang. Biol.* **2021**, *27*, 1504–1517. [[CrossRef](#)]
- Boehnke, D. Exploring the Thermal Microcosms at the Forest Floor—A Case Study of a Temperate Forest. *Atmos. Basel* **2021**, *12*, 503. [[CrossRef](#)]
- Rita, A.; Bonanomi, G.; Allevato, E.; Borghetti, M.; Cesarano, G.; Mogavero, V.; Rossi, S.; Saulino, L.; Zotti, M.; Saracino, A. Topography Modulates Near-Ground Microclimate in the Mediterranean Fagus Sylvatica Treeline. *Sci. Rep. UK* **2021**, *11*, 8122. [[CrossRef](#)] [[PubMed](#)]
- Christiansen, D.M.; Iversen, L.L.; Ehrlén, J.; Hylander, K. Changes in Forest Structure Drive Temperature Preferences of Boreal Understorey Plant Communities. *J. Ecol.* **2021**, *110*, 631–643. [[CrossRef](#)]
- Greiser, C.; Meineri, E.; Luoto, M.; Ehrlén, J.; Hylander, K. Monthly Microclimate Models in a Managed Boreal Forest Landscape. *Agric. For. Meteorol.* **2018**, *250*, 147–158. [[CrossRef](#)]
- Wolf, C.; Bell, D.M.; Kim, H.; Nelson, M.P.; Schulze, M.; Betts, M.G. Temporal Consistency of Undercanopy Thermal Refugia in Old-Growth Forest. *Agric. For. Meteorol.* **2021**, *307*, 108520. [[CrossRef](#)]
- Rull, V. Microrefugia. *J. Biogeogr.* **2009**, *36*, 481–484. [[CrossRef](#)]
- Reside, A.E.; Van Der Wal, J.; Phillips, B.L.; Shoo, L.P. Climate Change Refugia for Terrestrial Biodiversity. *Austral Ecol.* **2014**, *39*, 887–897. [[CrossRef](#)]
- Gavin, D.G.; Fitzpatrick, M.C.; Gugger, P.F.; Heath, K.D.; Sánchez, F.R.; DOBROWSKI, S.Z.; Hampe, A.; Hu, F.S.; Ashcroft, M.B.; Bartlein, P.J.; et al. Climate Refugia: Joint Inference from Fossil Records, Species Distribution Models and Phylogeography. *New Phytol.* **2014**, *204*, 37–54. [[CrossRef](#)] [[PubMed](#)]
- Maclean, I.M.D.; Hopkins, J.J.; Bennie, J.; Lawson, C.R.; Wilson, R.J. Microclimates Buffer the Responses of Plant Communities to Climate Change. *Glob. Ecol. Biogeogr.* **2015**, *24*, 1340–1350. [[CrossRef](#)]
- Morelli, T.L.; Daly, C.; Dobrowski, S.Z.; Dulen, D.M.; Ebersole, J.L.; Jackson, S.T.; Lundquist, J.D.; Millar, C.I.; Maher, S.P.; Monahan, W.B.; et al. Managing Climate Change Refugia for Climate Adaptation. *PLoS ONE* **2016**, *11*, e0159909. [[CrossRef](#)] [[PubMed](#)]
- Keppel, G.; Wardell-Johnson, G.W. Refugia: Keys to Climate Change Management. *Glob. Chang. Biol.* **2012**, *18*, 2389–2391. [[CrossRef](#)]
- Keppel, G.; Mokany, K.; Wardell-Johnson, G.W.; Phillips, B.L.; Welbergen, J.A.; Reside, A.E. The Capacity of Refugia for Conservation Planning under Climate Change. *Front. Ecol. Environ.* **2015**, *13*, 106–112. [[CrossRef](#)]
- Morelli, T.L.; Barrows, C.W.; Ramirez, A.R.; Cartwright, J.M.; Ackerly, D.D.; Eaves, T.D.; Ebersole, J.L.; Krawchuk, M.A.; Letcher, B.H.; Mahalovich, M.F.; et al. Climate-Change Refugia: Biodiversity in the Slow Lane. *Front. Ecol. Environ.* **2020**, *18*, 228–234. [[CrossRef](#)]

27. von Arx, G.; Pannatier, E.G.; Thimonier, A.; Rebetez, M. Microclimate in Forests with Varying Leaf Area Index and Soil Moisture: Potential Implications for Seedling Establishment in a Changing Climate. *J. Ecol.* **2013**, *101*, 1201–1213. [[CrossRef](#)]
28. Ashcroft, M.B.; Gollan, J.R. Moisture, Thermal Inertia, and the Spatial Distributions of near-Surface Soil and Air Temperatures: Understanding Factors That Promote Microrefugia. *Agric. For. Meteorol.* **2013**, *176*, 77–89. [[CrossRef](#)]
29. Maclean, I.M.D.; Suggitt, A.J.; Wilson, R.J.; Duffy, J.P.; Bennie, J.J. Fine-Scale Climate Change: Modelling Spatial Variation in Biologically Meaningful Rates of Warming. *Glob. Chang. Biol.* **2017**, *23*, 256–268. [[CrossRef](#)]
30. Davis, K.T.; Dobrowski, S.Z.; Holden, Z.A.; Higuera, P.E.; Abatzoglou, J.T. Microclimatic Buffering in Forests of the Future: The Role of Local Water Balance. *Ecography* **2019**, *42*, 1–11. [[CrossRef](#)]
31. Macek, M.; Kopecký, M.; Wild, J. Maximum Air Temperature Controlled by Landscape Topography Affects Plant Species Composition in Temperate Forests. *Landscape Ecol.* **2019**, *34*, 2541–2556. [[CrossRef](#)]
32. Williamson, J.; Slade, E.M.; Luke, S.H.; Swinfield, T.; Chung, A.Y.C.; Coomes, D.A.; Heroin, H.; Jucker, T.; Lewis, O.T.; Vairappan, C.S.; et al. Riparian Buffers Act as Microclimatic Refugia in Oil Palm Landscapes. *J. Appl. Ecol.* **2020**, *58*, 431–442. [[CrossRef](#)]
33. Lembrechts, J.J.; van den Hoogen, J.; Aalto, J.; Ashcroft, M.B.; de Frenne, P.D.; Kempainen, J.; Kopecký, M.; Luoto, M.; Maclean, I.M.D.; Crowther, T.W.; et al. Global Maps of Soil Temperature. *Glob. Chang. Biol.* **2022**. [[CrossRef](#)] [[PubMed](#)]
34. Zellweger, F.; de Frenne, P.D.; Lenoir, J.; Rocchini, D.; Coomes, D. Advances in Microclimate Ecology Arising from Remote Sensing. *Trends Ecol. Evol.* **2019**, *34*, 327–341. [[CrossRef](#)] [[PubMed](#)]
35. García, M.B.; Domingo, D.; Pizarro, M.; Font, X.; Gómez, D.; Ehrlén, J. Rocky Habitats as Microclimatic Refuges for Biodiversity. A Close-up Thermal Approach. *Environ. Exp. Bot.* **2020**, *170*, 103886. [[CrossRef](#)]
36. George, A.D.; Thompson, F.R.; Faaborg, J. Using LiDAR and Remote Microclimate Loggers to Downscale Near-Surface Air Temperatures for Site-Level Studies. *Remote Sens. Lett.* **2015**, *6*, 924–932. [[CrossRef](#)]
37. Keppel, G.; Robinson, T.P.; Wardell-Johnson, G.W.; Yates, C.J.; Niel, K.P.V.; Byrne, M.; Schut, A.G.T. A Low-Altitude Mountain Range as an Important Refugium for Two Narrow Endemics in the Southwest Australian Floristic Region Biodiversity Hotspot. *Ann. Bot.* **2017**, *119*, 289–300. [[CrossRef](#)]
38. Jucker, T.; Hardwick, S.R.; Both, S.; Elias, D.M.O.; Ewers, R.M.; Milodowski, D.T.; Swinfield, T.; Coomes, D.A. Canopy Structure and Topography Jointly Constrain the Microclimate of Human-Modified Tropical Landscapes. *Glob. Chang. Biol.* **2018**, *24*, 5243–5258. [[CrossRef](#)]
39. Stickley, S.F.; Fraterrigo, J.M. Understorey Vegetation Contributes to Microclimatic Buffering of Near-Surface Temperatures in Temperate Deciduous Forests. *Landsc. Ecol.* **2021**, *36*, 1197–1213. [[CrossRef](#)]
40. Stewart, S.B.; Elith, J.; Fedrigo, M.; Kasel, S.; Roxburgh, S.H.; Bennett, L.T.; Chick, M.; Fairman, T.; Leonard, S.; Kohout, M.; et al. Climate Extreme Variables Generated Using Monthly Time-Series Data Improve Predicted Distributions of Plant Species. *Ecography* **2021**, *44*, 626–639. [[CrossRef](#)]
41. Pardo, I.; Roquet, C.; Lavergne, S.; Olesen, J.M.; Gómez, D.; García, M.B. Spatial congruence between taxonomic, phylogenetic and functional hotspots: True pattern or methodological artefact? *Divers. Distrib.* **2017**, *23*, 209–220. [[CrossRef](#)]
42. Fawcett, S.; Sistla, S.; Calheiros, M.D.; Kahraman, A.; Reznicek, A.A.; Rosenberg, R.; von Wettberg, E.J.B. Tracking Microhabitat Temperature Variation with IButton Data Loggers. *Appl. Plant Sci.* **2019**, *7*, e01237. [[CrossRef](#)] [[PubMed](#)]
43. Fick, S.E.; Hijmans, R.J. WorldClim 2: New 1-km Spatial Resolution Climate Surfaces for Global Land Areas. *Int. J. Clim.* **2017**, *37*, 4302–4315. [[CrossRef](#)]
44. McGaughey, R. *FUSION/LDV: Software for LIDAR Data Analysis and Visualization 2009, Version 3.10*; USDA Forest Service: Washington, DC, USA, 2014; pp. 1–212.
45. Serrano-Notivol, R.; Beguería, S.; Saz, M.Á.; Longares, L.A.; de Luis, M. SPREAD: A high-resolution daily gridded precipitation dataset for Spain—An extreme events frequency and intensity overview. *Earth Syst. Sci. Data* **2017**, *9*, 721–738. [[CrossRef](#)]
46. Serrano-Notivol, R.; Beguería, S.; de Luis, M. STEAD: A high-resolution daily gridded temperature dataset for Spain, *Earth Syst. Sci. Data* **2019**, *11*, 1171–1188. [[CrossRef](#)]
47. Montealegre, A.L.; Lamelas, M.T.; de la Riva, J. A Comparison of Open-Source LiDAR Filtering Algorithms in a Mediterranean Forest Environment. *IEEE J. Sel. Top. Appl.* **2015**, *8*, 4072–4085. [[CrossRef](#)]
48. Evans, J.S.; Hudak, A.T. A Multiscale Curvature Algorithm for Classifying Discrete Return LiDAR in Forested Environments. *IEEE Trans. Geosci. Remote* **2007**, *45*, 1029–1038. [[CrossRef](#)]
49. Hijmans, R.J. Raster: Geographic Data Analysis and Modeling. R Package Version 3.1-13. 2020. Available online: <https://CRAN.R-project.org/package=raster> (accessed on 18 February 2022).
50. Boehner, J.; Antonic, O. Land-surface parameters specific to topo-climatology. In *Geomorphometry-Concepts, Software, Applications*; Hengl, T., Reuter, H., Eds.; Elsevier: Amsterdam, The Netherlands, 2008; Volume 33, pp. 195–226.
51. Jennings, S.; Brown, N.; Sheil, D. Assessing Forest Canopies and Understorey Illumination: Canopy Closure, Canopy Cover and Other Measures. *Int. J. Res.* **1999**, *72*, 59–74. [[CrossRef](#)]
52. Fox, J.F.; Wesberg, S. *An R Companion to Applied Regression*, 3rd ed.; Sage: Thousand Oaks, CA, USA, 2019.
53. Bartoń, K. MuMIn: Multi-Model Inference. R Package Version 1.46.0. 2020. Available online: <https://CRAN.R-project.org/package=MuMIn> (accessed on 25 February 2022).
54. Grömping, U. Relative Importance for Linear Regression in R: The Package Relaimpo. *J. Stat. Softw.* **2006**, *17*, 1–27. [[CrossRef](#)]
55. Gunton, R.M.; Polce, C.; Kunin, W.E. Predicting Ground Temperatures across European Landscapes. *Methods Ecol. Evol.* **2015**, *6*, 532–542. [[CrossRef](#)]

56. Ashcroft, M.B.; Gollan, J.R. Fine-Resolution (25 m) Topoclimatic Grids of near-Surface (5 Cm) Extreme Temperatures and Humidities across Various Habitats in a Large (200 × 300 Km) and Diverse Region. *Int. J. Climatol.* **2012**, *90*, 2134–2148. [[CrossRef](#)]
57. Meineri, E.; Hylander, K. Fine-Grain, Large-Domain Climate Models Based on Climate Station and Comprehensive Topographic Information Improve Microrefugia Detection. *Ecography* **2017**, *40*, 1003–1013. [[CrossRef](#)]
58. Gubler, M.; Henne, P.D.; Schwörer, C.; Boltshauser-Kaltenrieder, P.; Lotter, A.F.; Brönnimann, S.; Tinner, W. Microclimatic Gradients Provide Evidence for a Glacial Refugium for Temperate Trees in a Sheltered Hilly Landscape of Northern Italy. *J. Biogeogr.* **2018**, *45*, 2564–2575. [[CrossRef](#)]
59. Frey, S.J.K.; Hadley, A.S.; Johnson, S.L.; Schulze, M.; Jones, J.A.; Betts, M.G. Spatial Models Reveal the Microclimatic Buffering Capacity of Old-Growth Forests. *Sci. Adv.* **2016**, *2*, e1501392. [[CrossRef](#)]
60. Dobrowski, S.Z.; Abatzoglou, J.T.; Greenberg, J.A.; Schladow, S.G. How Much Influence Does Landscape-Scale Physiography Have on Air Temperature in a Mountain Environment? *Agric. For. Meteorol.* **2009**, *149*, 1751–1758. [[CrossRef](#)]
61. Aalto, J.; Riihimäki, H.; Meineri, E.; Hylander, K.; Luoto, M. Revealing Topoclimatic Heterogeneity Using Meteorological Station Data. *Int. J. Climatol.* **2017**, *37*, 544–556. [[CrossRef](#)]
62. de Frenne, P.D.; Lenoir, J.; Luoto, M.; Scheffers, B.R.; Zellweger, F.; Aalto, J.; Ashcroft, M.B.; Christiansen, D.M.; Decocq, G.; Pauw, K.D.; et al. Forest Microclimates and Climate Change: Importance, Drivers and Future Research Agenda. *Glob. Chang. Biol.* **2021**, *27*, 2279–2297. [[CrossRef](#)]
63. McCullough, I.M.; Davis, F.W.; Dingman, J.R.; Flint, L.E.; Flint, A.L.; Serra-Diaz, J.M.; Syphard, A.D.; Moritz, M.A.; Hannah, L.; Franklin, J. High and Dry: High Elevations Disproportionately Exposed to Regional Climate Change in Mediterranean-Climate Landscapes. *Landscape Ecol.* **2015**, *31*, 1–13. [[CrossRef](#)]
64. Reside, A.E.; Welbergen, J.A.; Phillips, B.L.; Wardell-Johnson, G.W.; Keppel, G.; Ferrier, S.; Williams, S.E.; Van Der Wal, J. Characteristics of Climate Change Refugia for Australian Biodiversity. *Austral Ecol.* **2014**, *39*, 887–897. [[CrossRef](#)]
65. Schut, A.G.T.; Wardell-Johnson, G.W.; Yates, C.J.; Keppel, G.; Baran, I.; Franklin, S.E.; Hopper, S.D.; Niel, K.P.V.; Mucina, L.; Byrne, M. Rapid Characterisation of Vegetation Structure to Predict Refugia and Climate Change Impacts across a Global Biodiversity Hotspot. *PLoS ONE* **2014**, *9*, e82778. [[CrossRef](#)]
66. Greiser, C.; Ehrlén, J.; Meineri, E.; Hylander, K. Hiding from the Climate: Characterizing Microrefugia for Boreal Forest Understory Species. *Glob. Chang. Biol.* **2019**, *26*, 32. [[CrossRef](#)] [[PubMed](#)]
67. Zellweger, F.; de Frenne, P.D.; Lenoir, J.; Vangansbeke, P.; Verheyen, K.; Bernhardt-Römermann, M.; Baeten, L.; Hédl, R.; Berki, I.; Brunet, J.; et al. Forest Microclimate Dynamics Drive Plant Responses to Warming. *Science* **2020**, *368*, 772–775. [[CrossRef](#)] [[PubMed](#)]
68. Lombaerde, E.D.; Vangansbeke, P.; Lenoir, J.; Meerbeek, K.V.; Lembrechts, J.; Rodríguez-Sánchez, F.; Luoto, M.; Scheffers, B.; Haesen, S.; Aalto, J.; et al. Maintaining Forest Cover to Enhance Temperature Buffering under Future Climate Change. *Sci. Total Environ.* **2021**, *810*, 151338. [[CrossRef](#)]
69. Norris, C.; Hobson, P.; Ibisch, P.L. Microclimate and Vegetation Function as Indicators of Forest Thermodynamic Efficiency. *J. Appl. Ecol.* **2012**, *49*, 562–570. [[CrossRef](#)]
70. Zellweger, F.; Coomes, D.; Lenoir, J.; Depauw, L.; Maes, S.L.; Wulf, M.; Kirby, K.J.; Brunet, J.; Kopecký, M.; Máliš, F.; et al. Seasonal Drivers of Understorey Temperature Buffering in Temperate Deciduous Forests across Europe. *Glob. Ecol. Biogeogr.* **2019**, *28*, 1774–1786. [[CrossRef](#)]
71. Oliver, T.; Roy, D.B.; Hill, J.K.; Brereton, T.; Thomas, C.D. Heterogeneous Landscapes Promote Population Stability. *Ecol. Lett.* **2010**, *13*, 473–484. [[CrossRef](#)]
72. Stein, A.; Gerstner, K.; Kreft, H. Environmental Heterogeneity as a Universal Driver of Species Richness across Taxa, Biomes and Spatial Scales. *Ecol. Lett.* **2014**, *17*, 866–880. [[CrossRef](#)]
73. Hylander, K.; Ehrlén, J.; Luoto, M.; Meineri, E. Microrefugia: Not for Everyone. *AMBIO* **2015**, *44*, 60–68. [[CrossRef](#)]